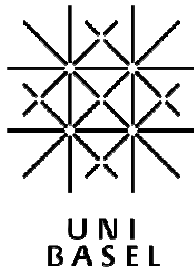


Synthesis and characterization of scratch resistant polyurethane clear coatings by incorporation of surface modified nanoparticles



Inauguraldissertation

zur

Erlangung der Würde eines Doktors der Philosophie
vorgelegt der
Philosophisch-Naturwissenschaftlichen Fakultät
der Universität Basel

von

Elisabeth Barna
aus Oberschützen, Österreich

Zürich, 2012



Namensnennung-Keine kommerzielle Nutzung-Keine Bearbeitung 2.5 Schweiz

Sie dürfen:



das Werk vervielfältigen, verbreiten und öffentlich zugänglich machen

Zu den folgenden Bedingungen:



Namensnennung. Sie müssen den Namen des Autors/Rechteinhabers in der von ihm festgelegten Weise nennen (wodurch aber nicht der Eindruck entstehen darf, Sie oder die Nutzung des Werkes durch Sie würden entlohnt).



Keine kommerzielle Nutzung. Dieses Werk darf nicht für kommerzielle Zwecke verwendet werden.



Keine Bearbeitung. Dieses Werk darf nicht bearbeitet oder in anderer Weise verändert werden.

- Im Falle einer Verbreitung müssen Sie anderen die Lizenzbedingungen, unter welche dieses Werk fällt, mitteilen. Am Einfachsten ist es, einen Link auf diese Seite einzubinden.
- Jede der vorgenannten Bedingungen kann aufgehoben werden, sofern Sie die Einwilligung des Rechteinhabers dazu erhalten.
- Diese Lizenz lässt die Urheberpersönlichkeitsrechte unberührt.

Die gesetzlichen Schranken des Urheberrechts bleiben hiervon unberührt.

Die Commons Deed ist eine Zusammenfassung des Lizenzvertrags in allgemeinverständlicher Sprache: <http://creativecommons.org/licenses/by-nc-nd/2.5/ch/legalcode.de>

Haftungsausschluss:

Die Commons Deed ist kein Lizenzvertrag. Sie ist lediglich ein Referenztext, der den zugrundeliegenden Lizenzvertrag übersichtlich und in allgemeinverständlicher Sprache wiedergibt. Die Deed selbst entfaltet keine juristische Wirkung und erscheint im eigentlichen Lizenzvertrag nicht. Creative Commons ist keine Rechtsanwalts-gesellschaft und leistet keine Rechtsberatung. Die Weitergabe und Verlinkung des Commons Deeds führt zu keinem Mandatsverhältnis.

Genehmigt von der Philosophisch-Naturwissenschaftlichen Fakultät
auf Antrag von

Prof. Dr. Wolfgang Meier
Prof. Dr. Andreas Taubert

Basel, den 22. Juni 2010

Prof. Dr. Martin Spiess
Dekan

Foreword and Acknowledgements

Starting my PhD I thought I knew perfectly well where it was leading me to – I had my topic and aim and a plan how to get there in three years' time.

In fact once on the road it was much more adventurous than I would have thought. I took short cuts that turned out to be detours and the most promising routes sometimes lead to dead ends. Natural disaster came over me when I needed it least but nevertheless had to be dealt with. But then I was also surprised by amazing findings and touched by the support and encouragement to find my way.

Looking back I was lucky to learn a lot for my future professional life but the more essential things were other than science. I learned how important it is to get back on track and that crossing the finishing line in the end depends upon so many little things falling into place. Above all, the success of any journey highly depends on your travel mates.

The work was directed by Prof. Dr. Wolfgang Meier and I thank him for scientific discussions, valuable advice and having so much patience with me.

Prof. Dr. Thomas Graule I would like to thank for giving me the opportunity to do my PhD at EMPA and to take part in an interesting CTI project which became a major part of this thesis. Many thanks go to my collaborators in this project: Dr. Andri Vital, Walter Koch, Nicolas Conté, Dr. Steffen Pilotek and Dr. Reiner Zimmer for the excellent collaboration and the fruitful discussions.

I thank my former colleagues at the High Performance Ceramics Lab and my PhD mates Dr. Sophie Duval, Dr. Juliane Heiber, Dr. Defne Bayraktar, Dr. Katja Lemster, Dr. Maryam Bahraini, Dr. Peter Ried, Daniel Wiedenmann, Dr. Marc Delporte and Jean Philippe Dellemann for living through all ups and downs of a young researcher's life. Hearty thanks go to Dr. Lucy Kind who I worked together with and who became a dear friend.

Lastly and most importantly I wish to thank my family for their unconditional love and support in all those years.

Abstract

The reinforcement of polymers by addition of fillers has been a field of research for some decades. The use of fillers in the nanometer scale, so called nanofillers, is relatively new though and has been intensively studied only since the 1990ies. Due to the high surface to volume ratio this class of fillers provides considerably more surface to interact with the polymer matrix than conventional fillers and significant improvement of properties can be achieved at relatively low filling rates. Additionally these fillers are suitable for application in transparent polymers such as coatings because in the ideal case of uniformly dispersed particles there is no interaction with incident light and thus no turbidity of the resulting composite material. Unfortunately, due to interparticle Van der Waals forces nanofillers show a high tendency to agglomerate with decreasing particle size and these agglomerates may reach several hundred nanometers in size.

In this work the reinforcement of different kinds of nanoparticles in transparent polyurethane coating compositions was studied, particularly with regard to scratch resistance of the resulting nanocomposite. Nanoparticles synthesized by flame spray synthesis, microemulsion polymerization and conventional aerosol process were employed as well as commercially available silica organosols. Some of these nanoparticles were surface modified with organosilanes to improve the interaction with the polymer matrix and provide for a uniform dispersion in the coating system. Surface modification with functional organosilanes bearing amino-, mercapto- or glycidoxy groups allow for reactive integration of the nanoparticles in the polyurethane network and thus enhance the mechanical properties. Also tailor made mixed oxide nanoparticles with a refractive index matched to that of the polymer system were synthesized via flame spray synthesis.

Nanoparticles were characterized by means of Transmission electron microscopy (TEM). The quality of organosilane surface modification was controlled with the help of Solid State ^{29}Si NMR and Thermogravimetric Analysis (TGA). The nanoparticles were incorporated in polyurethane coating formulations and films thereof applied on glass sheets. After curing at 180 °C the transparency of these films was determined using UV/vis spectroscopy. To check the particle dispersion within the coating layer ultramicrotomed cross-sections were investigated by TEM. The scratch behavior of the nanocomposite films was studied with the help of a Nano Scratch Tester (NST). Further investigations like Differential Scanning Calorimetry (DSC) and Dynamic Mechanical Thermal Analysis (DMTA) was performed on selected samples.

Table of Contents

1	Introduction	1
2	Objectives.....	7
3	Materials.....	9
	3.1. Polymer matrix.....	9
	3.2. Nanoparticles	9
	3.3. Organosilanes.....	10
4	Methods	11
	4.1. Characterization of nanoparticles and nanoparticle surface modification.....	11
	4.2. Characterization of nanocomposite coatings	12
	4.3. Scratch Testing.....	13
	4.3.1. The Nano Scratch Tester (NST)	14
5	Surface modification of nanoparticles for scratch resistant clear coatings.....	21
	5.1. Introduction	22
	5.2. Experimental.....	23
	5.2.1. Materials.....	23
	5.2.2. Functionalization.....	24
	5.2.3. Characterization.....	24
	5.3. Results and Discussion	24
	5.4. Conclusions	28
6	Scratch behaviour of polyurethane clear coatings reinforced with organosilane grafted nanoparticles	31
	6.1. Introduction	32
	6.2. Experimental.....	34
	6.2.1. Materials.....	34
	6.2.2. Surface modification of nanopowders	35
	6.2.3. Preparation of particle reinforced coatings	35
	6.2.4. Characterization of cured coatings	35
	6.3. Results	37

6.4. Discussion	43
6.4.1. Mechanical and thermal properties.....	43
6.4.2. Optical properties.....	44
6.5. Conclusion.....	45
7 Efficiency of commercially available silica organosols in the scratch resistance improvement of transparent polyurethane clear coatings	47
7.1 Introduction	48
7.2 Materials and Methods.....	48
7.3 Results and Discussion	49
7.4 Conclusion.....	51
8 Refractive index matching of silica/alumina mixed oxide nanoparticles for scratch resistant clear coatings	61
8.1. Introduction	62
8.2. Results and Discussion	64
8.2.1. Nanoparticle Synthesis and Characterization.....	64
8.2.2. Nanocomposite Coatings.....	68
8.3. Conclusion.....	68
8.4. Experimental.....	70
8.4.1. Flame Spray Synthesis	70
8.4.2. Particle Characterization.....	71
8.4.3. Preparation of coatings.....	72
8.4.4. Characterization of cured coatings	72
9 Conclusion	75
Curriculum vitae	

1 Introduction

Synthetic polymers have found their way to all areas of man's life since their invention in the 19th century and are practically omnipresent nowadays. A world without plastic goods has become hard to imagine. We do the shopping with Polyethylene bags, buy drinks in PET bottles, store our food in plastic bowls and wear functional clothing made of high tech synthetic fibers. Computers, sports equipment, furniture and innumerable other things in our daily life are made of polymeric materials. Also in the construction of cars, trains and planes there is a continuous trend to substitute metal and ceramic parts by polymers to save weight and reduce costs.

The consumption of polymers is growing steadily and has reached a worldwide value of 245 Mio Tons in 2007, 60 Mio Tons of which were produced in Europe. Two thirds of polymers produced today go into packaging and construction industries. Although a multitude of new polymers and copolymers showing impressive properties have been developed lately a major part of polymers used today are so called commodities or bulk polymers like polyethylene (PE), polypropylene (PP), polyvinylchloride (PVC) and polystyrene (PS).^[1] These polymers are known for a long time and show a restricted property range compared to engineering plastics or high performance plastics. In 1975 the polymer consumption of 27 Mio Tons was composed of 86 % bulk plastics, 14 % engineering plastics and less than 1 % high performance plastics. The forecast back then for 1996 predicted a growth of high performance and engineering plastics to be the major volumes of polymers consumed. Actually, the ratio of these three polymer groups is nowadays still in the same range like 1975 and the anticipated shift in the direction of high end polymers did not take place.^[2] There are ample applications in which high performance polymers or engineering polymers are required but these materials are also quite expensive compared to bulk polymers. Alternatively, bulk polymers can be modified by the use of additives and fillers leading to a significant improve of properties.^[3] Thus, bulk

1 Introduction

polymers can be adapted to fulfill a growing number of applications including some that were dominated by metals or ceramics.

The reinforcement of polymers by fillers has been a field of research for many years.^[3-6] With the help of incorporated particles, fibers and platelets characteristics like the mechanical, optical, thermal and electrical properties can be improved. Thus, the application spectrum of these polymers is expanded significantly and properties can be perfectly adjusted to the final application.

Fillers can generally be divided in active and inactive fillers. Inactive fillers are also called extenders and are used to dilute the polymer and reduce costs. Active fillers are coupled to the polymer matrix either via physical adhesion or chemical bonding and improve specific properties of the composite and thus often allow a tuning of properties for a special application. Fillers differ in size, shape and chemical nature and are often characterized by the aspect ratio which is the ratio of filler diameter or length to filler thickness. Regarding the size, fillers in polymers are classified as micro-fillers – exceeding 1 micrometer, submicron fillers – less than 1 micrometer, and nano-fillers – less than 100 nanometers. Concerning their shape fillers can roughly be divided in fibers, spheres and platelets. Another important parameter for the application in polymers is the specific surface area (SSA) indicating the surface area per gram. However, this number is often hard to interpret as in particular small filler particles tend to form agglomerates and thus only a fraction of the initial surface is available for interaction with the polymer matrix. The polymer at the interface to the filler particle is to some extent adsorbed on to the filler surface. This adsorbed polymer shows different properties than the bulk material. The thickness of this immobilized polymer fraction depends on the chemical nature of the filler and the polymer matrix but has a major impact on the properties of the reinforced composite material.^[4, 7, 8] Hence, nanofillers are particularly interesting as reinforcing additives because of their high surface to volume ratio which provides a large area for interaction with the polymer.^[9] That allows for good reinforcement of the polymer matrix even at low filling rates.

Whereas micro and submicron fillers have been in use in polymer formulations for a long time, nanoscale fillers are a relatively new class of fillers and have experienced a remarkable interest for the last two decades. Layered silicates, nanotubes and a variety of oxide nanoparticles are employed to improve polymer properties. Nanocomposites

based on layered silicates in Nylon 6 (PA6) were first reported on by Okada et. al.^[10-13] Layered silicates have been employed with great success in a variety of polymers since then.^[14-20] Various nanofiller/polymer combinations have been studied on and are often intended for a specific application.^[21-26] Additionally, the filler/polymer interaction can be improved by surface modification with functional organosilanes. Thus, filler particles can be reactively linked to the polymer matrix.^[27-29]

The field of nanocomposite research concentrating on the mechanical improvement of transparent polymers with no or negligible decline of optical properties is relatively new. The reinforcement of transparent polymer matrices without deterioration of optical properties has only become possible with the help of nanofillers. Conventional fillers in the micron or submicron range cause light scattering and the composite appears turbid. Because of their minor size which is smaller than the wavelength of visible light nanoscale fillers do not interfere with incident light. That only applies in the case of separated and uniformly dispersed nanoparticles. Unfortunately, nanoparticles tend to form agglomerates because of interparticle van der Waals forces resulting from the high specific surface. These agglomerates often are several hundred nanometers in size and therefore act like micron or submicron particles scattering the incident light and decreasing the nanocomposite's transparency.

Up to date only few studies focus on mechanical reinforcement of transparent polymers where the maintenance or improvement of the optical properties is a major issue.^[30-34] An enhancement of mechanical properties of transparent coatings is highly advantageous. Clear coatings are used as protection in multilayer configurations like car coatings but also as a finish on polymer parts such as bike and ski helmets, sports equipment and domestic devices to improve the physical appearance. In either application these coatings are subject to scratching and marring that reduce the attractiveness and the function of the goods.

In this work several approaches to improve the scratch resistance of polyurethane clear coatings while maintaining excellent transparency of the nanocomposite films are introduced.

To avoid agglomeration of particles and to ensure good compatibility and even chemical linking to the polymer matrix nanoparticles were surface modified with the

1 Introduction

help of organosilanes. The silanization procedure as well as the characterization of silane coating is described in **Chapter 5**.

The subsequent incorporation of coated and uncoated nanoparticles in the model polyurethane matrices and the characterization of the resulting nanocomposites are discussed in **Chapter 6**.

Furthermore, commercially available silica organosols and their effect on the scratch resistance and transparency was studied as described in **Chapter 7**.

In addition to improving the dispersion and integration of nanoparticles via surface modification, also mixed oxide nanoparticles with a tailored Refractive Index to match that of the polyurethane coating system were synthesized by Flame Spray Synthesis. Thus, light scattering is minimized and because of similar Hamaker constants also dispersion can be improved. That approach is explained and summarized in **Chapter 9**.

References

- [1] Plastics Europe, Brussels, Belgium 2009.
- [2] H. Dragaun, "Geschichte, Entwicklung und heutiger Stand der PE-Werkstoffe in der Gasversorgung", presented at *Kongress und Fachmesse Gas und Wasser*, Wien, 2006.
- [3] W. Hohenberger, *Kunststoffe International* **2005**, 95, 187.
- [4] R. N. Rothon, Ed. *Particulate-Filled Polymer Composites*, Rapra Technology Limited, Shrewsbury 2003.
- [5] M. Xanthos, Ed. *Functional Fillers for Plastics*, Wiley-VCH, Weinheim 2005.
- [6] J.-F. Gerard, *Fillers and Filled Polymers* **2001**, 169.
- [7] D. J. Kohls, G. Beaucage, *Curr. Opin. Solid State Mat. Sci.* **2002**, 6, 183.
- [8] G. Heinrich, M. Klüppel, T. A. Vilgis, *Curr. Opin. Solid State Mat. Sci.* **2002**, 6, 195.
- [9] L. Schadler, L. Brinson, W. Sawyer, *JOM* **2007**, 59, 53.
- [10] A. Okada, M. Kawasumi, A. Usuki, Y. Kojima, T. Kurauchi, O. Kamigaito, in *Polymer Based Molecular Composites*, Vol. 171 (Eds: D. W. Schaefer, J. E. Mark), Materials Research Soc, Pittsburgh 1990, 45.
- [11] A. Usuki, Y. Kojima, M. Kawasumi, A. Okada, T. Kurauchi, O. Kamigaito, *Abstr. Pap. Am. Chem. Soc.* **1990**, 200, 218.
- [12] Y. Kojima, A. Usuki, M. Kawasumi, A. Okada, T. Kurauchi, O. Kamigaito, *J. Polym. Sci. Pol. Chem.* **1993**, 31, 983.

- [13] Y. Kojima, A. Usuki, M. Kawasumi, A. Okada, Y. Fukushima, T. Kurauchi, O. Kamigaito, *J. Mater. Res.* **1993**, 8, 1185.
- [14] M. Ganter, W. Gronski, H. Semke, T. Zilg, R. Thomann, R. Muhlhaupt, *KGK-Kaut. Gummi Kunst.* **2001**, 54, 166.
- [15] P. B. Messersmith, E. P. Giannelis, *Chem. Mater.* **1993**, 5, 1064.
- [16] P. B. Messersmith, E. P. Giannelis, *Chem. Mater.* **1994**, 6, 1719.
- [17] M. S. Wang, T. J. Pinnavaia, *Chem. Mat.* **1994**, 6, 468.
- [18] C. Zilg, R. Mülhaupt, J. Finter, *Macromol. Chem. Physic.* **1999**, 200, 661.
- [19] B. Ahmadi, M. Kassiriha, K. Khodabakhshi, E. R. Mafi, *Prog. Org. Coat.* **2007**, 60, 99.
- [20] E. Barna, Thesis, Montanuniversität Leoben, 2001.
- [21] B. Wetzell, F. Hauptert, M. Qiu Zhang, *Compos. Sci. Technol.* **2003**, 63, 2055.
- [22] Z. S. Petrovic, I. Javni, A. Waddon, G. Bánhegyi, *J. Appl. Polym. Sci.* **2000**, 76, 133.
- [23] C. Chen, R. S. Justice, D. W. Schaefer, J. W. Baur, *Polymer* **2008**, 49, 3805.
- [24] X. Xu, B. Li, H. Lu, Z. Zhang, H. Wang, *Appl. Surf. Sci.* **2007**, 254, 1456.
- [25] S. C. Tjong, *Mat. Sci. Eng. R* **2006**, 53, 73.
- [26] P. Hajji, L. David, J. F. Gerard, J. P. Pascault, G. Vigier, *J. Polym. Sci. Pol. Phys.* **1999**, 37, 3172.
- [27] F. Bauer, H.-J. Glasel, U. Decker, H. Ernst, A. Freyer, E. Hartmann, V. Sauerland, R. Mehnert, *Prog. Org. Coat.* **2003**, 47, 147.
- [28] D. V. Szabó, D. Vollath, *Adv. Mater.* **1999**, 11, 1313.
- [29] A. Hunsche, U. Görl, A. Müller, M. Knaack, T. Göbel, *KGK-Kaut. Gummi Kunst.* **1997**, 51, 525.
- [30] V. Khrenov, M. Klapper, M. Koch, K. Müllen, *Macromol. Chem. Physic.* **2005**, 206, 95.
- [31] H. Schulz, L. Mädler, S. E. Pratsinis, P. Burtscher, N. Moszner, *Adv. Funct. Mater.* **2005**, 15, 830.
- [32] L. Mädler, F. Krumeich, P. Burtscher, N. Moszner, *J. Nanopart. Res.* **2006**, 8, 323.
- [33] H. Althues, J. Henle, S. Kaskel, *Chem. Soc. Rev.* **2007**, 36, 1454.
- [34] S. H. Stelzig, M. Klapper, K. Müllen, *Adv. Mater.* **2008**, 20, 929.

2 Objectives

The study of the main parameters influencing the scratch resistance of nanoparticle reinforced transparent polymer coatings is the aim of this work. Based on model polymer systems the influence of different nanoparticles on the the scratch behaviour is investigated. Additionally, the transparency of the resulting nanocomposite films is to maintain a level higher than 90 % transmission relative to the unfilled coating.

The Parameters studied in this work are:

- **particle size:**
10 – 100 nm
- **organosilane surface modification:**
4 different functional and non functional silanes
- **synthesis route of nanoparticles:**
Aerosol Process, Flame Spray Synthesis, Micro Emulsion Polymerisation
- **pre-treatment of nanoparticles:**
dry nanopowder and silica organosols
- **chemical composition:**
silica, alumina and mixed oxide nanoparticles

3 Materials

3.1. Polymer matrix

As polymer matrix for our study two different 2-pack polyurethane coating formulations were chosen. These two formulations vary by the OH-content of the polyester polyol binder Desmophen. In all three cases a polyisocyanate, Desmophen N3300, was used as a hardener. Properties of binder and hardener are listed in Table 1. Formulations were cured by the addition of a stoichiometric amount of hardener to a mixture of polyester polyol and nanoparticles.

Table 1: Properties of the polyester polyole binders

Name	Function	Structure	Functional group [wt.%]
Desmophen 800*	binder	highly branched	OH 8.6 ± 0.3
Desmophen 1100*	binder	branched	OH 6.5 ± 0.5
Desmodur N3300*	hardener	HDI-Trimer	NCO 21.8 ± 0.3

*Bayer MaterialScience, Germany

3.2. Nanoparticles

The nanoparticles used in this work are of different synthesis routes and show a wide variation of properties. Some of them were surface modified in this work with the help of organosilanes whereas others were already delivered having a surface modification. A detailed list of the nanoparticles is given in

Table 2: Properties of nanoparticles

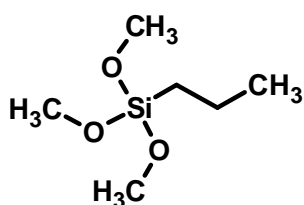
Name	Producer	Synthesis	Oxide	Primary particle size [nm]
Aerosil OX50	Degussa	Aerosil Process	SiO ₂	40
Aeroxide AluC	Degussa	Aerosil Process	Al ₂ O ₃	13
MOx	EMPA	Flame Spray Synthesis	SiO ₂ /Al ₂ O ₃	20 - 100
IME	University Basel	Inverse Micro Emulsion	SiO ₂	100

Table 3: Properties of commercially available silica organosols

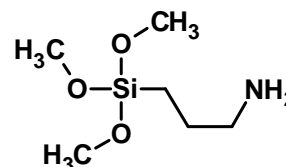
Name	Producer	Primary particle size [nm]	SiO ₂ loading [wt.%]	Solvent base	pH [-]
Nanopol XP21	Hanse Chemie	20	50	BuAc	3.5
Nissan MIBK-ST	Nissan Chemicals	10-15	30.5	MIBK	4.0
Highlink NanO G	Clariant	25	45	MIBK	3.5

3.3. Organosilanes

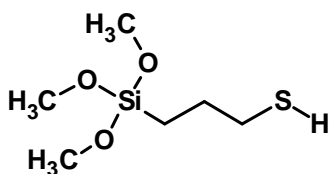
Four different methoxy silanes (Figure 1) were used to modify the surface of the nanoparticles in order to facilitate a uniform dispersion in the coating system and to reactively link the particles to the polymer network. Thus, propyltrimethoxy silane is employed to improve the particle dispersion and the physical adsorption of polymer on the particle surface. Surface modification with aminopropyl-, mercaptopropyl- and glycidoxypropyl silane are aiming at chemically linking the particle via surface coating to the polymer matrix.



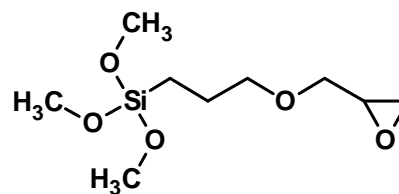
Propyltrimethoxy silane (PTMS)



Aminopropyl trimethoxy silane (APTMS)



Mercaptopropyl trimethoxy silane (MPTMS)



Glycidoxypropyl trimethoxy silane (GPTMS)

Figure 1: Functional silanes used for the surface modification of nanoparticles.

4 Methods

4.1. Characterization of nanoparticles and nanoparticle surface modification

Analysis of the particle morphology was performed by means of a **transmission electron microscopy (TEM)** (Philips CM 30, Philips, Eindhoven, Netherlands). A few milligrams of a powder were dispersed in 10 to 15 ml of isopropanol (>99.5 %, Fluka, Switzerland), and a few drops of the dispersion were applied on a copper grid coated with a carbon film (200 mesh, Plano GmbH, Wetzlar, Germany) and dried in a drying oven at 60 °C.

The specific surface area (SSA) of the flame synthesized powders was determined by a five-point N₂ adsorption isotherm applying the **BET (Brunauer-Emmett-Teller) method** (Beckman-Coulter SA3100). Prior to measurement the powder samples were degassed for three hours at 200 °C under flowing nitrogen to remove adsorbed water from the particle surface. From the specific surface area the BET-equivalent particle diameter d_{BET} (Sauter diameter) can be back-calculated assuming monomodal and spherical particles.

X-ray diffraction (XRD) was used to determine the phase composition of the powders. The analysis was performed with a Siemens D500 instrument. Diffraction patterns were recorded from 20° to 80° 2 θ angles using Ni-filtered CuK α radiation.

Refractive index (RI) of the powders was determined using the Becke Line Method. Powder grains were embedded in immersion oils of known refractive index (Cargille Labs, USA). When focused in a light microscope a light seam at the edge of the grain can be observed and by defocusing the light seam moves either into or out of the grain. By increasing the distance between object and objective the seam moves to the material with higher refractive index and to the one having lower refractive index by reducing the distance. That way the refractive indices of immersion oil and powder can be matched iteratively until no movement of the light seam can be observed any more.

4 Methods

Then the refractive index of the powder in question corresponds with the refractive index of the immersion oil. The accuracy of measurement is given by the step size and accuracy of immersion oils used and was 0.002 in this work.

Thermogravimetric analysis (TGA) was carried out on a Mettler Toledo TGA/SDTA 851 to determine the organic content bound to the particle surface. A heating rate of 10 K/min in the range between 30 and 800 °C was chosen. In addition to silane modified powder, raw oxides were also measured to correct for the mass loss of grafted powder by the mass loss of raw powder.

Cross polarization, magic angle spinning ^{29}Si NMR spectra were recorded using a Bruker Avance-400 NMR spectrometer at a magnetic field of 9.4 T on a 7 mm double resonance CP-MAS probe-head applying mixing times of 3 ms at a mixing frequency of 31.2 kHz (MAS rate: 3000 Hz).

4.2. Characterization of nanocomposite coatings

UV/vis transmission measurements were carried out using a UV/vis spectrophotometer (Cary 50, Varian Inc.). Coating formulations were applied on microscope slides and cured like described above. The transmission of these samples was measured in the range between 300 and 800 nm using a specimen holder for slides.

For **transmission electron microscopy (TEM)** coating samples were embedded and ultramicrotomed to slices of 45 nm. These slices were placed on copper grids and investigated using a Philips EM CM 100 microscope.

Glass transition temperature (T_g) of nanocomposite films was determined by **Differential Scanning Calorimetry (DSC)** using a DSC 7 (Perkin Elmer) in the range between -20 to 60 °C and a heating rate of 20 C/min.

Dynamic Mechanical Thermal Analysis (DMTA) was performed on nanocomposite films using an ATM3 (Myrenne GmbH, Germany) in torsion mode at a testing frequency of 1.0 Hz with automatic data acquisition. Tests were carried out on rectangular samples of thickness between 0.22 and 0.33 mm in a temperature range between -100 and 150 °C.

4.3. Scratch Testing

A variety of scratch testing methods are employed to judge the susceptibility of material surfaces to scratches. In most applications scratches do not influence the performance of the part in question but cause a major loss in attractiveness. In particular sports equipment is often not handled carefully and thus subject of scratch and mar damage.

In general scratch testing methods can be divided in

- multiple scratch methods and
- single scratch methods.

In multiple scratch testing methods the specimen surface is scratched simultaneously multiple times by devices like grains of sand, wires of steel wool or bristles of brushes. These tests are often oriented on later applications like car coatings where scratching by dirt and brushes during car wash is simulated by the Car Wash Lab Apparatus, Amtec Kistler, Germany^[1]. Here coating samples are placed under a rotating brush for a certain time and quartz powder can be added to simulate dirt particles. The scratch or mar resistance is determined by measuring the gloss of the samples before and after testing. Another often used example is the Taber Abraser Test, Taber Industries, New York, United States^[2-4]. A disk shaped specimen is mounted on the Taber Abraser and two turning wheels of arbitrary material are brought in contact with the specimen and then the specimen table is rotated a certain number of times. There are several standardized wheels available. When finished the weight difference is determined to judge the scratch/wear resistance of the material.

In the second group of methods a single scratch is introduced into the specimen's surface using one single tip. Thus parameters like applied load and scratch depth can be varied and resulting deformation of the surface can be monitored. Results can be directly related to the adjusted values. The scratch tips of this kind of testing devices vary in several orders of magnitude. While the Universal Scratch Hardness Tester 430 P-I, Erichsen, Germany works with tip radii of up to 3 mm the single scratch testers with the smallest tip radii are Atomic Force Microscopes with tip sizes down to a few nanometers^[3, 5]. In between these two there are several other testing machines with tip sizes adjusted to the kind of scratching relevant for application.

4 Methods

One of those single scratch testing methods is the Nano Scratch Tester, CSM Instruments, Switzerland, which was used for scratch testing the nanocomposite coatings produced in this thesis.

4.3.1. The Nano Scratch Tester (NST)

In order to judge the sensitivity of a surface to scratch deformation a scratch is introduced into the specimen's surface with a defined tip under a certain normal load and speed. The resulting tangential force, penetration depth and residual depth after viscoelastic recovery are recorded. Additionally the scratch is examined using a light microscope that is mounted on the Nano Scratch Tester. Thus different specimen can be compared in terms of scratch resistance.

The NST consists of the indenter which is covered, a light microscope with a camera and a specimen holder that is mounted on a moving table that can be arranged in x, y and z axis. For testing a specimen is mounted on the specimen holder and a clean and plane area for the scratch testing is selected using the microscope. The tip is brought into contact with the specimen's surface and the test started.

For our tests a diamond indenter with a tip radius of $2\ \mu\text{m}$ was used. The scratches induced with this size of tip are visible by the naked eye and can be described as scratches that typically appear during the normal handling of goods and are commonly observed on parts like sports helmets, sports goggles, household devices and mobile phones.

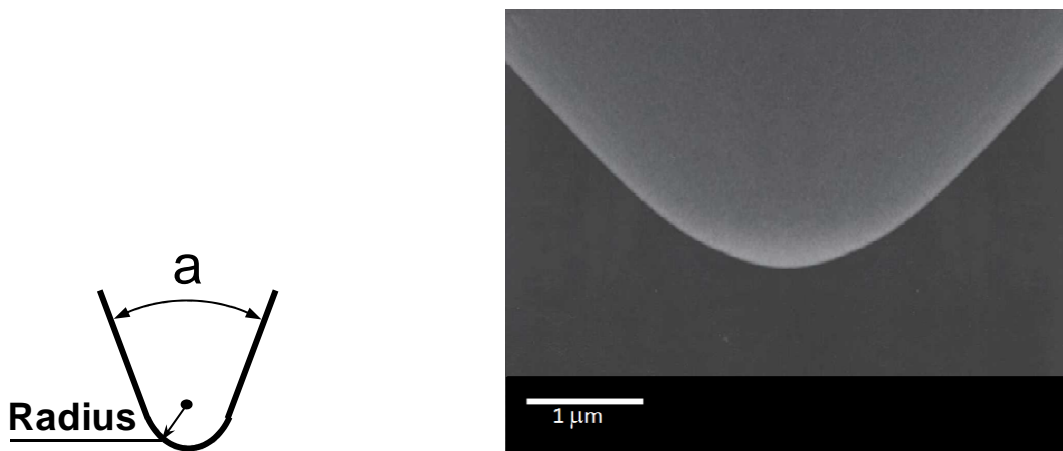


Figure 1: SEM picture of the scratch tip with a radius of $2\ \mu\text{m}$ and an opening angle of 90°

The principle of testing is shown in Figure 2. The indenter is drawn over the surface with the beforehand adjusted load applied and thus a scratch introduced in the surface of the specimen.

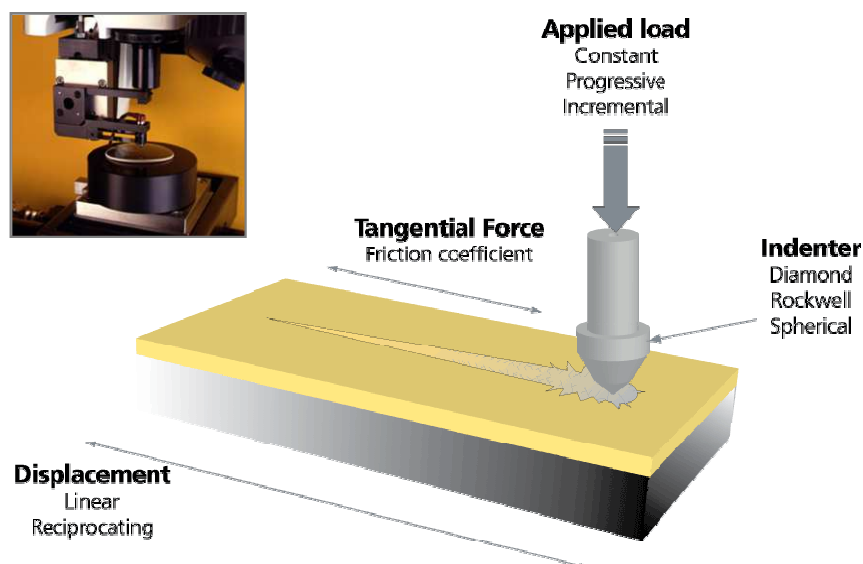


Figure 2: Scratch tip and specimen mounting table in close-up view and working principle^[6]

The load selected for the test is applied on the specimen via a double cantilever beam as shown in Figure 3. The applied load is controlled via the so-called “force feedback control loop”. The force applied is measured online via a displacement sensor and with the help of a piezo element the force is constantly adjusted to the value selected for the test. That way any unevenness of the specimen surface is compensated and the applied load during the test is exactly like planned. The load can be applied either as constant load, progressive load or incremental load, respectively.

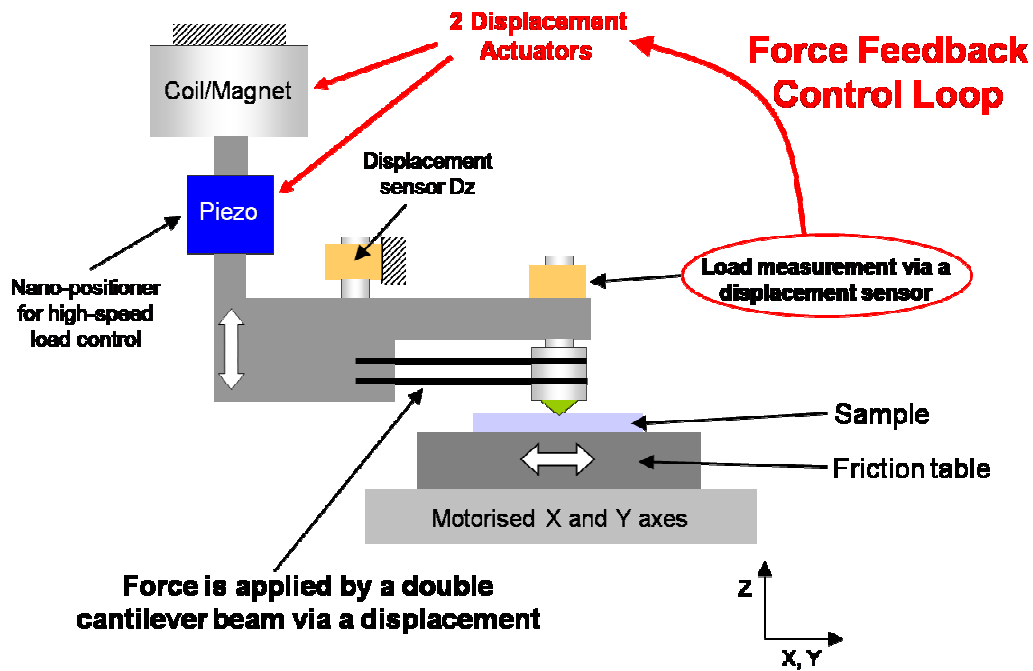


Figure 3: Working principle of the Nano Scratch Tester^[6]

The scratch test consists of three phases: pre-scan, scratch and post-scan. In the pre-scan phase, before the actual scratch testing, the surface topography is recorded with a negligible load applied to the indenter. This step is necessary to calculate the “real” penetration depth and residual depth after testing by subtraction of the pre-scan values from the measured depth. Then in the second step the actual scratch test is performed with the selected parameters. In this phase the tangential force and penetration depth are recorded. In the last phase the specimen table automatically goes back to the starting position and the post-scan is performed, measuring the residual depth. This step is particularly important for polymers because of their viscoelastic behavior. For the practical application of the tested coatings the residual depth is more important than the penetration depth because the residual depth represents the permanent damage induced in the specimen and is the reason for the loss of gloss and attractiveness. A typical diagram of a scratch test is shown in Figure 4.

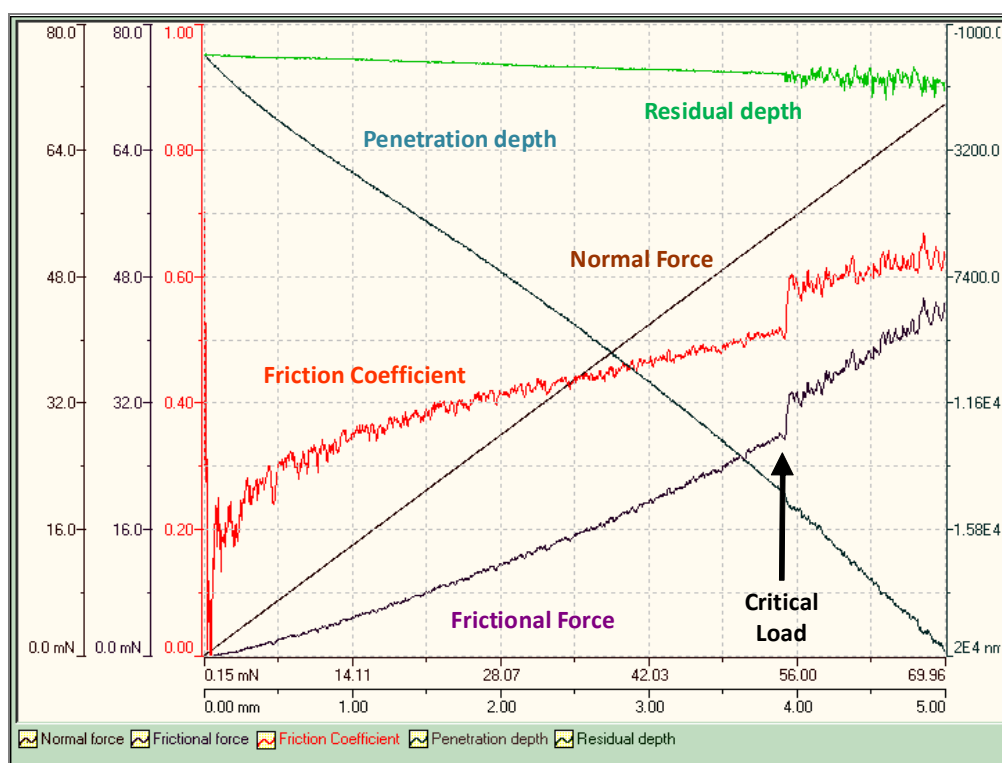


Figure 4: Diagram of the forces recorded during Nano Scratch Testing: Normal Force (brown line) Frictional Force (purple line), Friction Coefficient (red line), Penetration depth (petrol line) and residual depth (green line)

A scratch typically starts with elastic and plastic deformation of the specimen and formation of a pile up of material on both sides of the scratch path. With increasing normal force the deformation induced by the scratch tip is exceeding the tear strength of the sample material so cracks are formed (Figure 5). The occurrence of those cracks can directly be related to a step in the frictional force curves of the corresponding diagram, indicating the value for the critical load. The results for residual depth are evaluated in the post scan after the scratch testing. All rating of scratch resistance in this work is based on the critical load and residual dept describing the force necessary for scratch deformation and the ability of the material to recover.

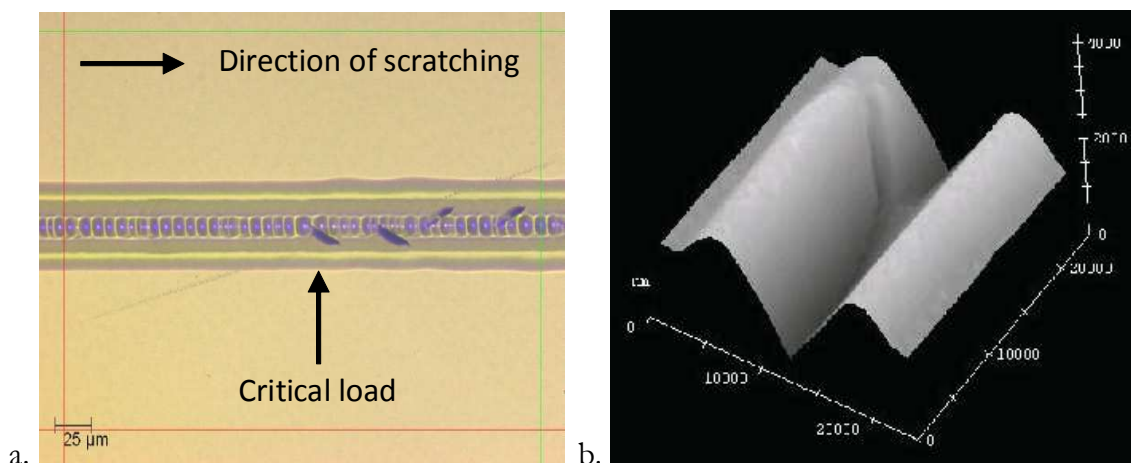


Figure 5: Image of a scratch path, indicating the occurrence of cracks when the critical load is exceeded (a) and AFM image of a cross section of a scratch path (b).^[6]

Different models are proposed in literature to describe the mechanisms involved in scratch deformation.^[7-13] However, these models are only applicable for a specific combination of material, scratch tip and test equipment because the scratch resistance is not a material specific parameter but a result of the testing parameters and environment. Still, results obtained with a specific equipment can be compared and used in the development of scratch resistant surfaces.

References

- [1] M. Osterhold, G. Wagner, *Prog. Org. Coat.* **2002**, 45, 365.
- [2] S. Sepeur, N. Kunze, B. Werner, H. Schmidt, *Thin Solid Films* **1999**, 351, 216.
- [3] H.-J. Gläsel, F. Bauer, H. Ernst, M. Findeisen, E. Hartmann, H. Langguth, R. Mehnert, R. Schubert, *Macromol. Chem. Physic.* **2000**, 201, 2765.
- [4] N. G. Salleh, H. J. Gläsel, R. Mehnert, *Radiat. Phys. Chem.* **2002**, 63, 475.
- [5] M. Spírková, M. Slouf, O. Bláhová, T. Farkacová, J. Benesová, *J. Appl. Polym. Sci.* **2006**, 102, 5763.
- [6] N. Conté, *Nano Scratch Tester (NST)*, 2007.
- [7] R. R. Thridandapani, A. Mudaliar, Q. Yuan, R. D. K. Misra, *Mat. Sci. Eng. A-Struct.* **2006**, 418, 292.
- [8] P. J. Burnett, D. S. Rickerby, *Thin Solid Films* **1987**, 154, 403.
- [9] J. L. Bucaille, E. Felder, G. Hochstetter, *Wear* **2001**, 249, 422.
- [10] J. S. S. Wong, H.-J. Sue, K.-Y. Zeng, R. K. Y. Li, Y.-W. Mai, *Act. Mater.* **2004**, 52, 431.

- [11] I. Demirci, C. Gauthier, R. Schirrer, *Thin Solid Films* **2005**, 479, 207.
- [12] C. Gauthier, A. L. Durier, C. Fond, R. Schirrer, *Tribology International* **2006**, 39, 88.
- [13] R. D. K. Misra, R. Hadal, S. J. Duncan, *Acta Mater* **2004**, 52, 4363.

5

Surface modification of nanoparticles for scratch resistant clear coatings*

Abstract

The incorporation of inorganic nanoscale particles into an organic matrix is of interest in many applications. Specific combinations of properties in coatings such as transparency and wear resistance can be obtained by the addition of nanoparticles. The interface between particle and polymer matrix plays an important role as a well integrated filler provides better mechanical reinforcement. When grafted with silanes heaving a reactive group, particles can be bound covalently to the polymer matrix via silane surface modification. Silica, alumina and titania nanopowders were surface modified using 3-aminopropyltrimethoxysilane. The quality of silane modification was characterised by solid state ^{29}Si NMR and TGA.

* E. Barna, D. Rentsch, B. Bommer, A. Vital, O. von Trzebiatowski, T. Graule, *Kautschuk Gummi Kunststoffe* **2007**, 60, 49.

5.1. Introduction

Nanoscale inorganic particles have gained wide interest as active fillers for polymers in the last decade. Various kinds of nanoparticles are being employed to improve polymer performance. Due to their high specific surface area (SSA) even at low reinforcement values impressive improvement of mechanical properties such as tensile strength, wear and scratch resistance can be achieved [1, 2].

In transparent polymer systems such as clear coatings and glass substitution polymers nanoscale fillers allow for reinforcement without altering the transparency of the matrix since nanoparticles are too small to cause scattering of visible light [3-5]. Most efforts to date have concentrated on UV- or thermally curable lacquers. However, in the case of coating polymers, these two materials possess some major disadvantages in the use as coating materials for polymer parts: polymers are usually rather sensitive to thermal exposure and therefore substrates may distort during curing of the clear coating. Furthermore, UV-curable coatings are suitable for flat parts, but reliable curing becomes complicated with three dimensional parts because of problems with non-uniform irradiation. In this work we concentrate on 2-pack polyurethane coatings that can be cured at room temperature and are an alternative to the above-mentioned lacquer types because no further treatment is required after application.

An important problem to be addressed in order to achieve good optical quality is the uniformity of particle dispersion. Due to their hydrophilic nature, oxidic nanoparticles like silica are hard to disperse homogeneously in bulk polymers. A method to overcome this limitation is the surface modification of particles with organosilanes. They render the powder surface hydrophobic and additionally, offer the advantage to serve as a linking molecule between particle surface and polymer matrix if the reactive group of the silane is matched to the polymer. Here 3-aminopropyltrimethoxysilane was used. The amino group reacts with the isocyanate hardener and that way links the particles to the polymer matrix. To ensure optimum integration of surface modified filler particles into the polymer network the quality of the silane shell has to be clarified. In the present work we describe the surface modification of four different oxidic nanoparticles and the characterisation of the resulting silane layer.

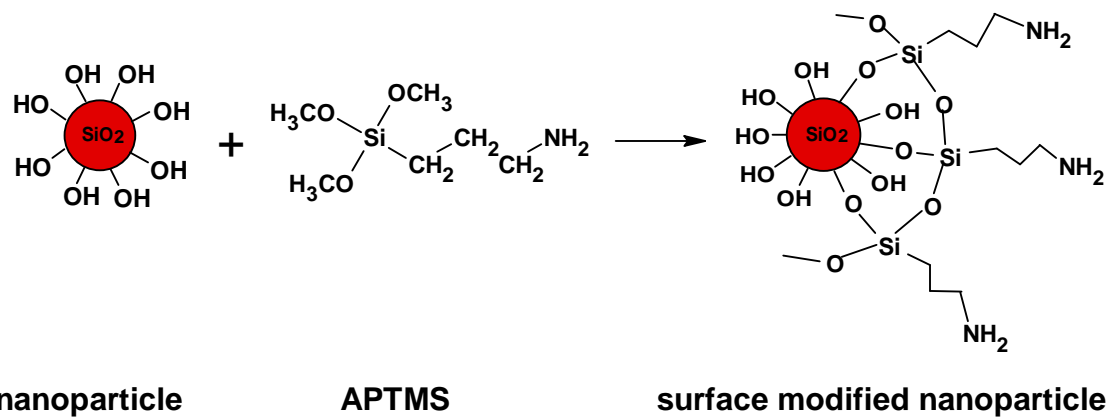


Figure 1: Idealized picture of APTMS surface grafted silica particle

5.2. Experimental

5.2.1. Materials

Silica (Aerosil OX50), alumina (Aeroxide Alu C) and titania (Aeroxide P25) were obtained from Degussa AG, Frankfurt. Properties of nanopowders are summarized in Table 1. Prior to use all powders were dried for 24 h at 180°C under vacuum. 3-Aminopropyltrimethoxysilane (APTMS) purchased at ABCR was used as received, methyl isobutyl ketone (MIBK) and ethanol were of technical grade.

Table 1: Properties of oxide nanopowders and mass loss determined by TGA

Oxide		Specific Surface Area (SSA)	OH group density	APTMS per 50 g oxide	Mass loss	Silane loading (calc.)
		[m ² /g]	[μmol/m ²]	[g]	[%]	[μmol/m ²]
Aerosil OX50	SiO ₂	50	4.65 [6]	2.1	1.30	4.48
Aeroxide P25	TiO ₂	50	8.96 [7]	4.0	0.54	1.86
Aeroxide Alu C	Al ₂ O ₃	100	assumed to be ~5	4.5	2.51	4.33
Aerosil 150	SiO ₂	150	4.65 [6]	6.3	3.39	3.90

5.2.2. Functionalisation

50 g of powder were dispersed in 200 g of MIBK using ultrasound for 10 min. The required amount of APTMS was calculated assuming 1 mol silane for 1 mol silanol groups of particle surface. Values for each substrate are given in Table 1. After silane addition the suspension was refluxed by intensive stirring for 24 h at 40 °C.

For solid state NMR measurements and thermogravimetric analysis 50 g of dispersion was ultra-centrifuged and washed twice with ethanol and then dried at 110 °C under vacuum for 24 h.

5.2.3. Characterisation

Cross polarization, magic angle spinning ^{29}Si NMR spectra were recorded using a Bruker Avance-400 NMR spectrometer at a magnetic field of 9.4 T on a 7 mm double resonance CP-MAS probe-head applying mixing times of 3 ms at a mixing frequency of 31.2 kHz (MAS rate: 3000 Hz).

Thermogravimetric analysis (TGA) was carried out on a Mettler Toledo TGA/SDTA 851 to determine the organic content bound to the particle surface. A heating rate of 10 K/min in the range between 30 and 800 °C was chosen. In addition to silane modified powder, raw oxides were also measured to correct for the mass loss of grafted powder by the mass loss of raw powder.

5.3. Results and Discussion

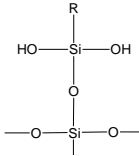
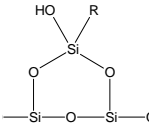
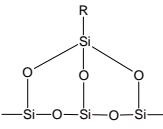
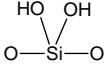

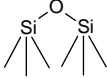
When trialkoxysilane is added to the oxide/MIBK dispersion, first the methoxy groups are hydrolysed and these bind to hydroxyl groups on the particle surface in a further step. Hydrolysed silanes also react with each other and form siloxane (Si-O-Si) bonds that may not be bound to the oxide surface and stay in solution while centrifugation. Only organosilane covalently bound to the particle surface provides for optimum filler integration in the polymer matrix.

^{29}Si CP MAS NMR is an adequate method to show the quality of silane bonds on the oxide surface [8-10]. Alkoxysilanes are able to form mono(T1)-, bi(T2)- and tri(T3)-

dental structures with oxidic surfaces (Table 2) that typically show peaks in the -45...-50 ppm, -55...-60 ppm and -65...-70 ppm regions, respectively.

The ^{29}Si MAS NMR spectra shown in Figure 2 prove that the silanisation reagent is bound to the particle surfaces. However, no conclusions can be drawn from the size of the peak area, since the CP-MAS experiments performed normally do not provide this information. On silica, T^2 and T^3 structures were observed, whereas on alumina and titania mainly bidental linking to the organosilane was noticed. The second group of peaks in the spectrum of the functionalized silica is assigned to geminal and free silanols at -90 ppm and -100 ppm, respectively.

Table 2: ^{29}Si chemical shifts of surface modified silica [11]

Monodental structure (T^1)	Bidental structure (T^2)	Tridental structure (T^3)	Geminal silanols Q^2	Free silanols Q^3	Siloxane Q^4
-45...-50 ppm	-55...-60 ppm	-65...-70 ppm	-90 ppm	-100 ppm	-110...-120 ppm
					

The amounts of organosilane attached to the nanopowder surfaces were quantitatively determined by thermogravimetric analysis. The blank values of the appropriate non-treated oxides were subtracted from these data (Table 1). A drop in mass starting around 300 °C is evident for all modified powders, whereas this phenomenon was not observed for raw powder. Therefore, it can be attributed to the release of the ligand.

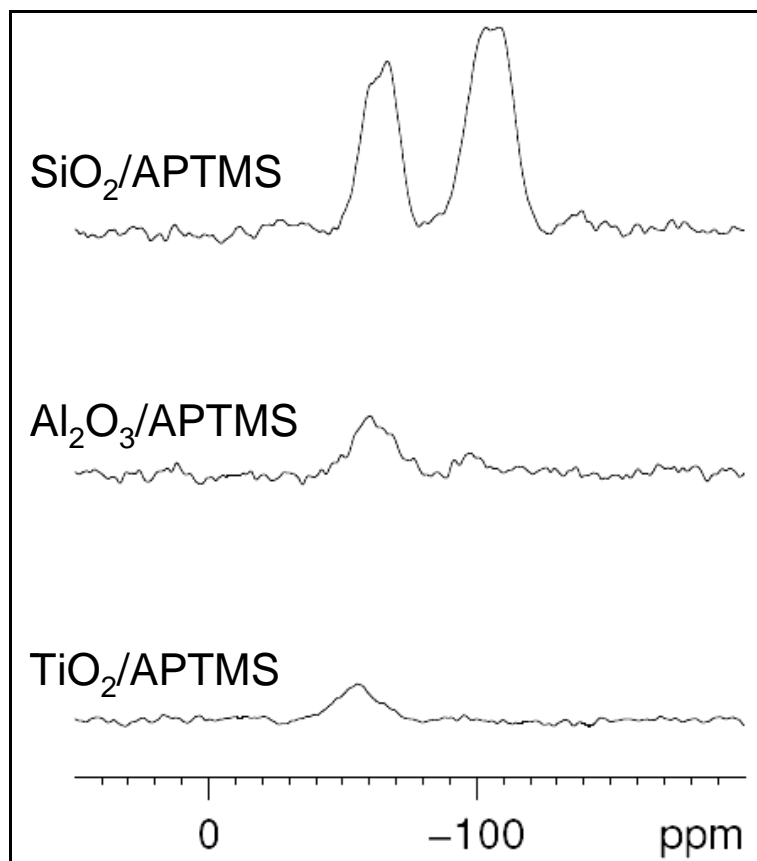


Figure 2: ^{29}Si CP-MAS NMR spectra of APTMS modified inorganic oxides

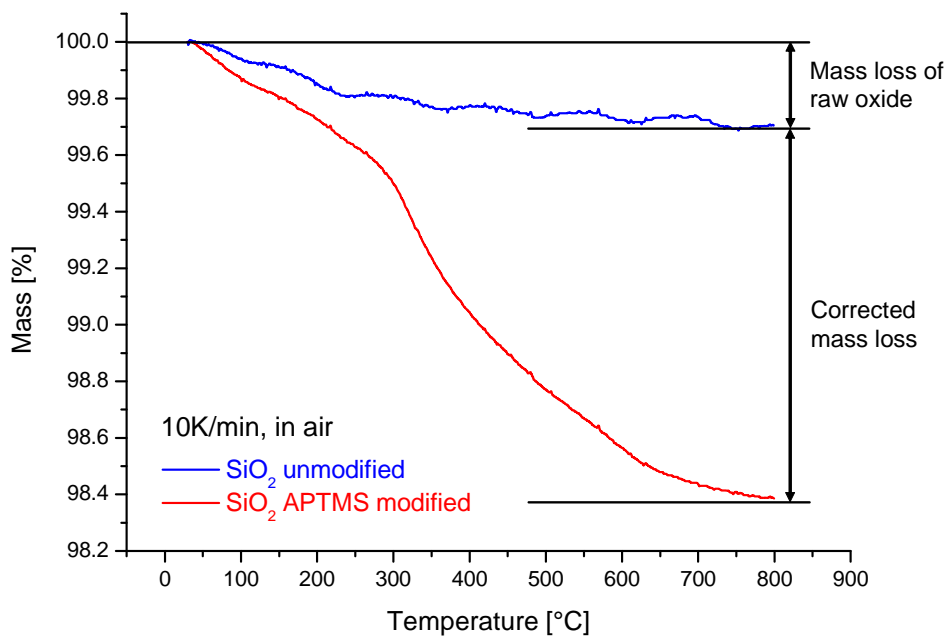


Figure 3: Correction of mass loss of surface modified powder by mass loss of raw powder

The theoretical loading of silane was calculated to be 1.6 wt.% for Aerosil OX50 grafted with APTMS assuming that all silane provided during the reaction formed covalent bonds with silanol groups on the particle surface. This value is in good correlation with TGA results for Aerosil OX50 and also Aerosil 150 having three times higher surface area and corresponding values for mass loss. Also the theoretical value for silane density on the surface was calculated from TGA data. Results are given in Table 1 and correspond very well with initial OH group density for silica and alumina nanopowder and a monolayer structure (Figure 5) of silane could be assumed. However, taking also the NMR data for silica into account it is evident that besides the bi- and tridentate linked silane there are also free silanols present. Thus the model of a silane shell consisting of 3D linked silanes around the particles (Figure 5) is more likely than a monolayered structure. The silane loadings achieved for titania are relatively low but there is nevertheless a silane layer on titania nanopowder.

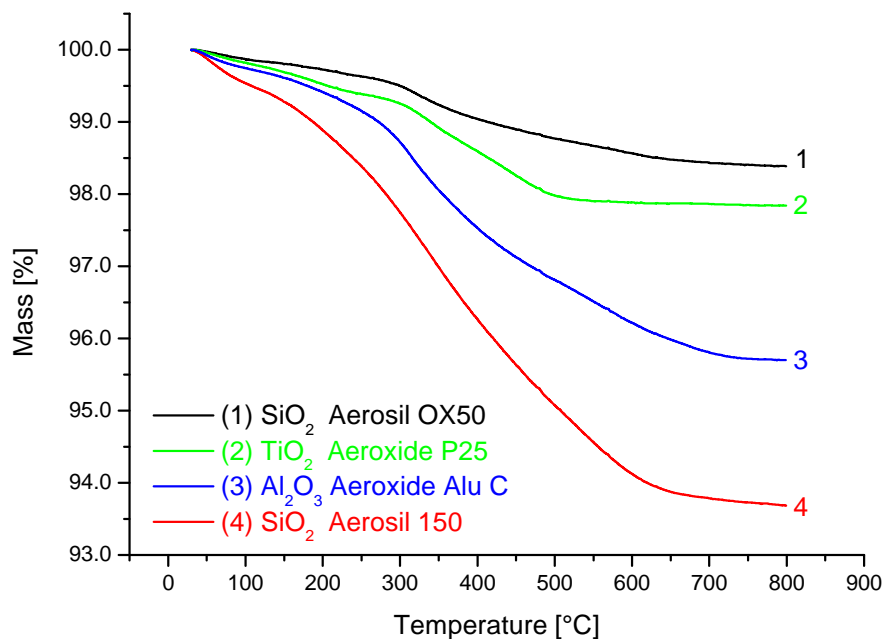


Figure 4: Mass loss of APTMS grafted oxide surfaces determined by TGA

5.4. Conclusions

Surface modification of silica, alumina and titania nanopowder with 3-Aminopropyltrimethoxysilane was accomplished and the existence of mono-, bi- and tridental structures of silanes on the particle surface was shown with ^{29}Si solid state MAS NMR. Furthermore the mass of organosilane bound to the powder was determined by TGA measurements and the theoretical silane loading was calculated from these values. Silica and alumina nanopowder show high loading and hence good chemical linking to polymer matrix is expected in further studies whereas titania surface bear less silane groups to form bonds with reactive sites in the polymer matrix. For the latter oxide an optimisation of silanisation procedure is recommended.

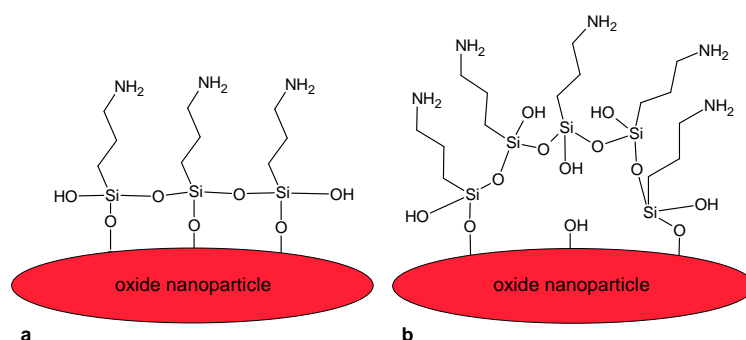


Figure 5: Possible silane structures on nanopowder surface: (a) monolayer and (b) 3D shell-like structure

Acknowledgements

Financial support by CTI (commission for technology and innovation) is kindly acknowledged (project KTI 7351.2).

References

- [1] C. Zilg, R. Mülhaupt, J. Finter, *Macromolecular Chemistry and Physics* **1999**, 200, 661.
- [2] B. Wetzels, F. Hauptert, M. Qiu Zhang, *Composites Science and Technology* **2003**, 63, 2055.
- [3] V. Khrenov, M. Klapper, M. Koch, K. Müllen, *Macromolecular Chemistry and Physics* **2005**, 206, 95.

- [4] F. Bauer, H.-J. Gläsel, U. Decker, H. Ernst, A. Freyer, E. Hartmann, V. Sauerland, R. Mehnert, *Progress in Organic Coatings* **2003**, 47, 147.
- [5] S. Sepeur, N. Kunze, B. Werner, H. Schmidt, *Thin Solid Films* **1999**, 351, 216.
- [6] in *Degussa AG, Schriftenreihe Pigmente*, Degussa AG, Frankfurt 1988.
- [7] T. Rentschler, *Farbe&Lack* **2000**, 106, 62.
- [8] F. Bauer, H. Ernst, U. Decker, M. Findeisen, H.-J. Gläsel, H. Langguth, E. Hartmann, R. Mehnert, C. Peuker, *Macromolecular Chemistry and Physics* **2000**, 201, 2654.
- [9] M. Luechinger, R. Prins, G. D. Pirngruber, *Microporous and Mesoporous Materials* **2005**, 85, 111.
- [10] E. Barna, B. Bommer, J. Kursteiner, A. Vital, O. v. Trzebiatowski, W. Koch, B. Schmid, T. Graule, *Composites Part A: Applied Science and Manufacturing* **2005**, 36, 473.
- [11] G. Engelhardt, H. Koller, in *Solid State NMR II: Inorganic Matter*, Vol. 31 (B. Blümich), Springer, Berlin, 1994.

6

Scratch behavior of polyurethane clear coatings reinforced with organosilane grafted nanoparticles*

Abstract

The aim of the present work was to elucidate the influence of nanoparticles on the scratch behavior of polyurethane clear coatings. Commercially available nanoparticles were surface modified with different organosilanes to ensure good dispersion in the coating film and to allow reactive linking to the polymer matrix. Scratch behavior of coating films was investigated using a CSM Nano Scratch Tester (NST). UV/vis spectra were recorded to control light transmission. Glass transition temperature was determined using differential scanning calorimetry (DSC). Transmission electron microscopy (TEM) was performed to investigate nanocomposite morphology. A considerable improvement of scratch behavior was achieved at low filler loadings along with good optical properties. Additionally, it was found that surprisingly good enhancement can be achieved by using raw, non surface modified nanoparticles.

* E. Barna, G. Hünnebeck, T. Graule, W. Meier, *to be submitted*.

6.1. Introduction

Polymers are found in a constantly increasing number of everyday objects due to their good processability and relatively low price. Unfortunately, polymer surfaces are particularly prone to scratch deformation. Already very fine scratches result in an objectionable decay of outside appearance of such polymer parts.

The reinforcement of bulk polymers with the help of particulate fillers is a common technique to broaden and optimise mechanical properties for specific applications. In recent years nanoparticles have opened a new field of polymer reinforcement. Various kinds have been employed successfully as active fillers in polymers [1, 2]. Due to their high specific surface area and thus high interaction with the polymer matrix, significant improvement of mechanical properties such as tensile strength, wear and scratch resistance can be achieved even at low loading rates.

In transparent applications such as clear coating systems nanoscale fillers are particularly interesting because they offer the potential of improving mechanical properties without deterioration of optical properties. Additionally optical properties of the polymer matrix, e.g. the refractive index, can be influenced by adequate nanoparticles. At best nanoparticles are dispersed uniformly in a transparent matrix and hence do not cause scattering of light and thus loss of transparency [3, 4].

Unfortunately, nanoparticles tend to form agglomerates due to high specific surface area and high interparticle Van der Waals forces. Thus these particles are hard to disperse in a matrix system. Dispersion and stabilization of such particles in solvents and polymer resins are often improved by surface modification with organosilanes bearing reactive and non reactive end groups [5]. The schematic of such a surface modification is shown in Figure 1. In the case of two component polyurethanes surface modification featuring reactive end groups such as amino, mercapto and glycidoxy can chemically react with a resin component, in our case either the polyol binder or the isocyanate hardener.

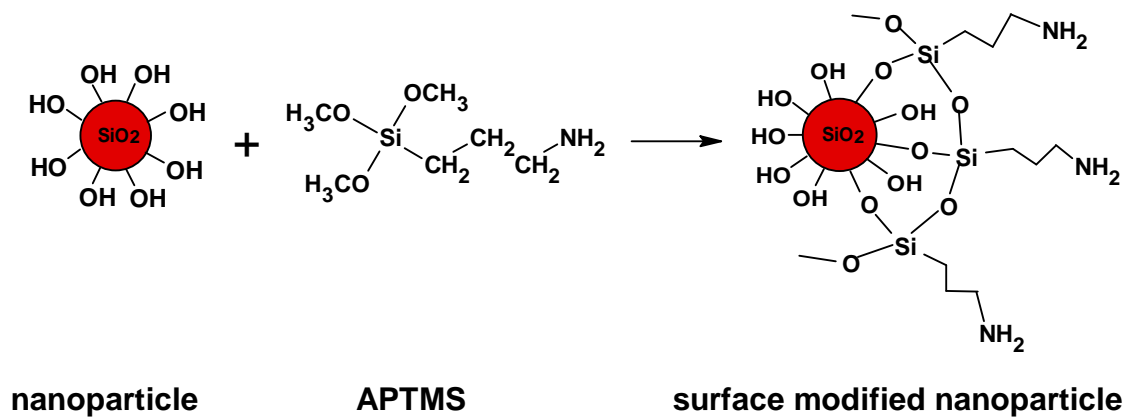


Figure 1: Surface modification of silica nanoparticles with 3-aminopropyltrimethoxysilane.

Silanes with reactive end groups facilitate the integration of particles into the resin network by chemical reaction of silane end groups with the polymer (Figure 2). This leads to active reinforcement of the polymer matrix by creation of additional cross linking. Non reactive silanes only allow for a physical adaptation to the polymer without chemical reaction. Hence the interface between particle and polymer matrix plays an important role, as a well integrated filler provides for better mechanical reinforcement.

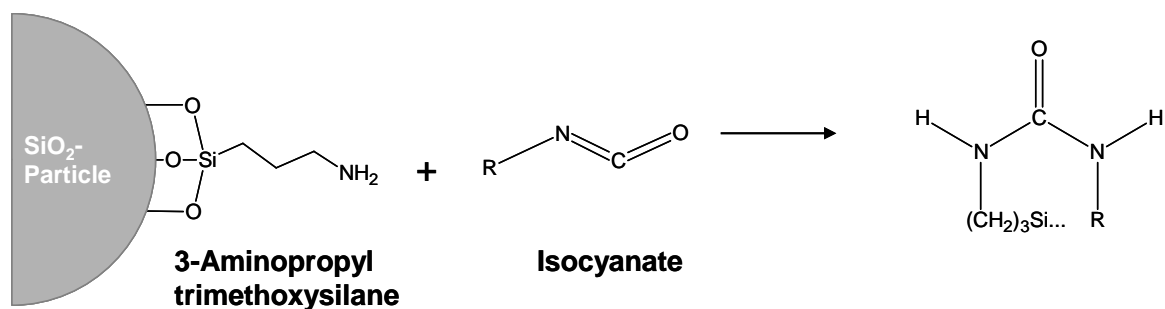


Figure 2: Schematic of surface amino groups reacting with isocyanate hardener.

In this work the scratch behavior of transparent 2 pack polyurethane coatings was the property to improve. Quantification and comparison of scratch resistance or scratch behavior in general is elusive due to a variety of existing test methods interrelated with the different fields of application of such materials. Results from different tests cannot be easily compared.

In general these tests differ in the tip size of the scratching medium varying from an AFM tip to pencil tips in a pencil hardness tester. Methods can also be divided into single and multi scratch tests. Multi scratch methods like steel wool scratching and

6 Scratch behavior

Taber Abraser (Taber Industries) produce good results for application but do not allow a direct correlation with compound morphology. Alternatives are single scratch methods. Here the sample surface is scratched with a single tip with a certain load. The acting forces and the scratch depth are recorded and the scratch path is subsequently examined. We chose a single scratch testing method, namely the Nano Scratch Tester (NST) to enable a correlation of the scratch behavior with the morphology of our coating samples.

Understanding the influence of surface modified and non modified oxidic nanoparticles on the scratch behavior of polyurethane clear coatings was a main focus of our work. Due to the fact that the price of a polymer compound is a crucial parameter in polymer industry in this study only commercially available and therefore relatively low priced nanoparticles were used.

6.2. Experimental

6.2.1. Materials

Silica (Aerosil OX50) and alumina (Aeroxide Alu C) were obtained from Evonik Industries AG, Germany. 3-Amino propyltrimethoxy silane (APTMS), Propyltrimethoxy silane (PTMS), 3-Mercaptopropyltrimethoxysilane (MPTMS) and 3-Glycidoxy propyltrimethoxy silane (GPTMS) were purchased from ABCR and used as received. Methyl isobutyl ketone (MIBK) and ethanol were of technical grade. Prior to use all powders were dried for 24 h at 180°C under vacuum. Polyurethane binders Desmophen 1100 and hardener Desmodur N3300 were obtained from Bayer AG. Ditinbutyllaureate (DBTL) was supplied by Basler Lacke AG.

Table 1: Properties of nanoparticles used

Name	Chemical name	Specific surface area, SSA	Primary particle size[6]	OH group density [$\mu\text{mol}/\text{m}^2$]
Aerosil OX50	SiO_2	50 ± 15	40	4,65
Aeroxide AluC	Al_2O_3	100 ± 15	13	assumed to be 5

6.2.2. Surface modification of nanopowders

50 g of nanopowder were dispersed in 200 g of MIBK using ultrasound for 10 min. The required amount of silane was calculated assuming 1 mol silane for 1 mol silanol groups on particle surface. Aerosil OX50 has a OH-group density of $4.65 \mu\text{mol}/\text{m}^2$ [7]. Aeroxide AluC is assumed to be in the same range due to similar production process. After silane addition the suspension was refluxed under intensive stirring for 24 h at 40°C . The procedure was described in more detail before [8]. For the preparation of coating samples the dispersions of surface modified silica particles in MIBK were used without any further purification.

6.2.3. Preparation of particle reinforced coatings

The nanoparticle/MIBK dispersion was mixed with the binder system and treated with ultrasound. Then redundant solvent was evaporated if necessary. In the following step the stoichiometric amount of hardener and catalyst were added and the formulation was homogenized by intensive stirring. Films were applied on glass sheets by doctor blade coating. Nanocomposite coatings containing filler degrees of 6, 10 and 20 vol.%, respectively were prepared. Coatings were cured for 12 h at 80°C . All produced compositions are listed in Table 2 along with corresponding mechanical properties and glass transition temperature.

6.2.4. Characterization of cured coatings

Scratch tests were performed using a Nano Scratch Tester (NST) from CSM Instruments SA. The principle of the NST is shown in Figure 3. A scratch tip of a known radius geometry is drawn over a sample surface with a certain load and speed. To eliminate the influence of surface structure a prescan is performed on the scratch path. During scratch testing the penetration depth and friction force are recorded. After the scratching a post scan is performed to determine the residual depth (r_d) of the scratch which gives information of the proportion of plastic to elastic deformation. For our samples the progressive load test was chosen starting at 10 mN and then increasing the load with 20 mN/mm. The test was stopped after breakdown of the coating film. The force at breakdown of the coating film is called the critical load (l_c). Three runs

6 Scratch behavior

were performed for each sample and the median is shown here. All tests were performed at a temperature of 21 °C. The residual depth (r_d) was evaluated at certain loads (30, 50, 100 mN). As scratch resistance is a combination of low residual depth and high critical load these values are depicted in an extra diagram.

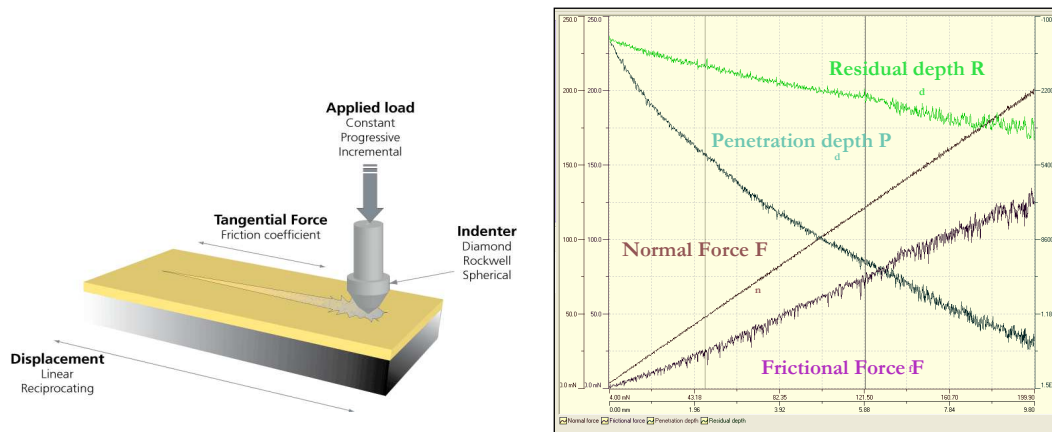


Figure 3: Schematic of the Nano Scratch Test (left) and a typical diagram recorded during a scratch test.

UV/vis transmission measurements were carried out with a UV/vis spectrophotometer (Cary 50, Varian Inc.). Coating formulations were applied on microscope slides and cured like described above. The transmission of these samples was measured in the range between 300 and 800 nm using a specimen holder for slides. Measured curves are given in % transmission of the unfilled coating film which was set to be 100%.

For Transmission electron microscopy (TEM) coating samples were embedded and ultramicrotomed to slices of 45 nm. These slices were placed on copper grids and investigated using a Philips EM CM 100 microscope.

Glass transition temperature (T_g) of nanocomposite films was determined by Differential Scanning Calorimetry using a DSC 7 (Perkin Elmer) in the range between (-20 °C) to (+60 °C) and a heating rate of 20 C/min.

6.3. Results

The critical load and residual depth values were recorded from NST measurements. Figure 4 shows critical load and glass transition temperature of silica reinforced samples. The critical load was raised significantly by incorporation of 6 vol.% silica nanoparticles (composition OX50-6, Figure 4). A rise of the filling degree to 10 vol.% did not further improve the critical load but lowered it remarkably. Values for 10 vol.% are still higher than for the unfilled coating. Incorporating 20 vol.% of non modified silica particles results in better reinforcement compared to 10 vol.% but lower than 6 vol.%. The high critical load for sample OX50-6 indicates the possibility of the hardener reacting with OH-groups on the particle surface.

Table 2: List of all produced samples, giving the exact composition (e.g. OX50-APTMS-10 indicates silica Aerosil OX50 with aminopropylsilane surface modification and a volume fraction of 10 vol.%) and the values measured for critical load, residual depth and glass transition temperature.

Coating composition	Critical load, l_c [mN]	Standard Deviation [mN]	Residual depth, r_d [μm]	Glass transition temperature, T_g [$^{\circ}\text{C}$]
unfilled DP1100	98.15	7.19	1.4	15.4
OX50-6	178.16	4.07	1.4	27.5
OX50-10	118.71	2.24	4.7	12.0
OX50-20	148.41	2.09	2.8	27.2
OX50-APTMS-10	134.39	2.13	1.6	17.7
OX50-APTMS-20	111.58	7.68	1.2	15.7
OX50-PTMS-10	107.63	0.42	1.1	11.6
OX50-GPTMS-10	149.39	4.92	1.2	12.2
OX50-GPTMS-20	112.67	1.18	2.0	16.9
OX50-MPTMS-6	191.42	8.44	2.0	28.5
OX50-MPTMS-10	140.50	1.99	1.3	27.3
OX50-MPTMS-20	147.55	4.70	2.5	25.8
AluC-6	200.42	5.92	1.9	25.7
AluC-10	159.66	1.87	2.6	24.4
AluC-APTMS-6	174.78	0.78	1.4	19.2
AluC-APTMS-10	161.44	1.81	2.4	18.6
AluC-GPTMS-6	213.27	3.99	2.4	26.1
AluC-GPTMS-10	161.51	6.86	2.5	-

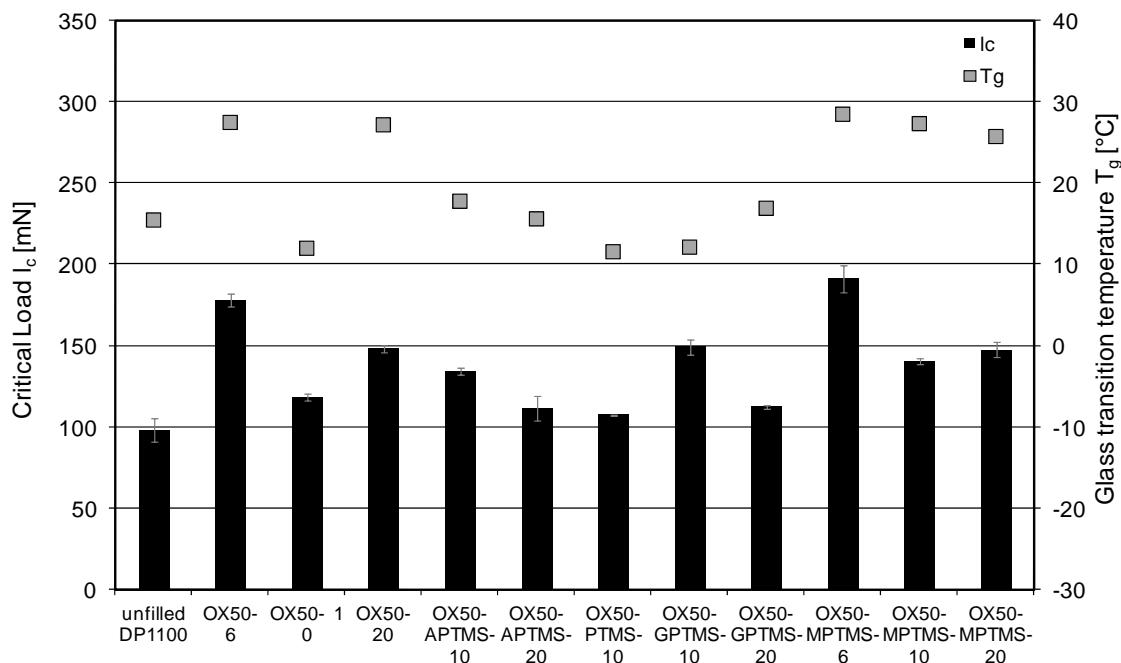


Figure 4: Critical load (I_c) and Glass transition temperature (T_g) of coating compounds reinforced with different volume fractions of silane coated and uncoated silica nanoparticles.

Among silane modified particles improvement is best for particles that were treated with silanes bearing reactive end groups such as amino, glycidoxy or mercapto groups that can react with one of the polyurethane components. Highest values for critical load were obtained by the coating composition OX50-MPTMS-6 containing 6 vol.% of silica nanoparticles that were surface modified with mercapto silane (MPTMS). The incorporation of 20 vol.% nanoparticles again lowered the critical load almost to the level of unfilled coating films. Least enhancement was found for PTMS modified silica. This might be due to the fact that PTMS is not able to react with the coating components and hence causes no active reinforcement.

Glass transition temperatures of samples with silica incorporated are shown with corresponding critical loads in Figure 4. Nanocomposites filled with surface modified and non modified silica particles show enhanced critical loads if T_g is higher than testing temperature. Except for samples OX50-GPTMS-20, there is also a tendency for coatings with higher T_g to achieve higher critical loads.

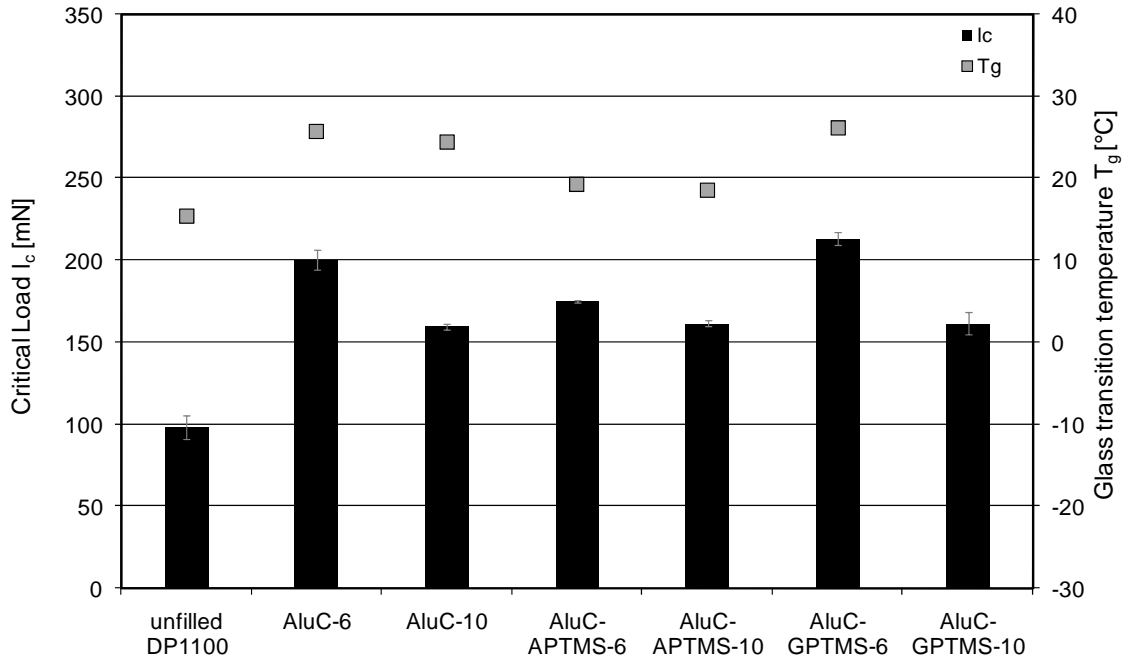


Figure 5: Critical load (l_c) and Glass transition temperature (T_g) of coating compounds reinforced with different volume fractions of silane coated and uncoated alumina nanoparticles.

Values for the critical load of coating compositions reinforced with surface modified and non modified alumina nanoparticles are shown in Figure 5. The improvement of the critical load compared to the unfilled coating was achieved for all alumina containing samples and values are higher than those for silica reinforced samples. Again, non surface modified nanoparticles show surprisingly high values (AluC-6) which might also indicate a reaction of the polymer with OH-groups on the particle surface. Highest values were obtained by incorporation of 6 vol.% of alumina nanoparticles that were surface modified using GPTMS. As seen before in series with silica nanoparticles, higher critical loads are observed for compositions comprising 6 vol.% than for 10 vol.%.

A strong dependency of the critical load on the glass transition temperature is found like before in series with silica nanoparticles. Also T_g is decreasing when the filler loading is increased. T_g for sample AluC-GPTMS-10 could not be measured because the film disintegrated upon removal from the glass plate and thus representative results could not be guaranteed.

6 Scratch behavior

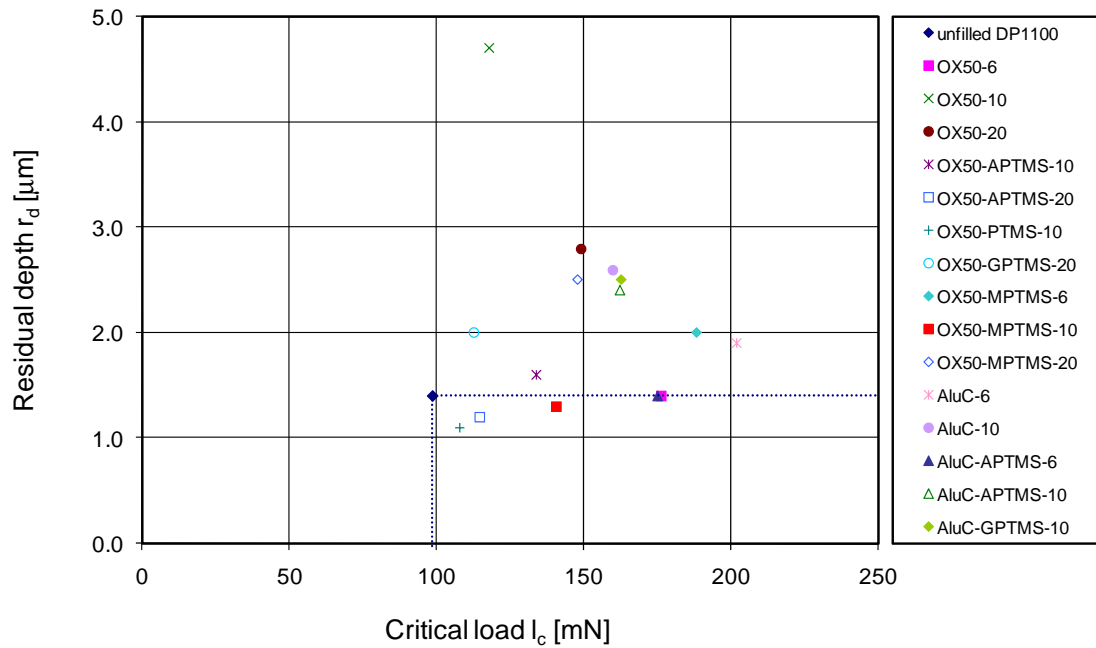


Figure 6: Critical load versus residual depth of all tested samples. The area of improved scratch resistance is marked by blue line.

When the critical load values are plotted versus the corresponding residual depth, coating compositions with improved scratch resistance are located in the lower right part of the diagram shown in Figure 6. As shown before the critical load was improved for all nanoparticle containing compositions. Opposite to findings concerning the critical load in the case of the residual depth only few samples show improved behavior presented by smaller values for the residual depth in the diagram.

Five compositions (located in the blue rectangle in Figure 6) can be considered to be more scratch resistant than the unfilled coating composition. For the sample filled with 10 vol.% PTMS-modified silica both the critical load and the residual depth were improved slightly which is also true for the sample filled with 20 vol.% of silica modified with APTMS. The incorporation of 10 vol.% MPTMS-modified silica nanoparticles increases the critical load significantly but the residual depth is only improved marginally. The best improvement of the critical load without deterioration of elastic behavior is found for two compositions incorporating 6 vol.% of either unmodified silica or the same amount of APTMS-modified alumina particles. All other samples show higher residual depths.

Transmission electron microscopy was performed to investigate the quality of particle dispersion in general and also throughout the cross section of the coating film.

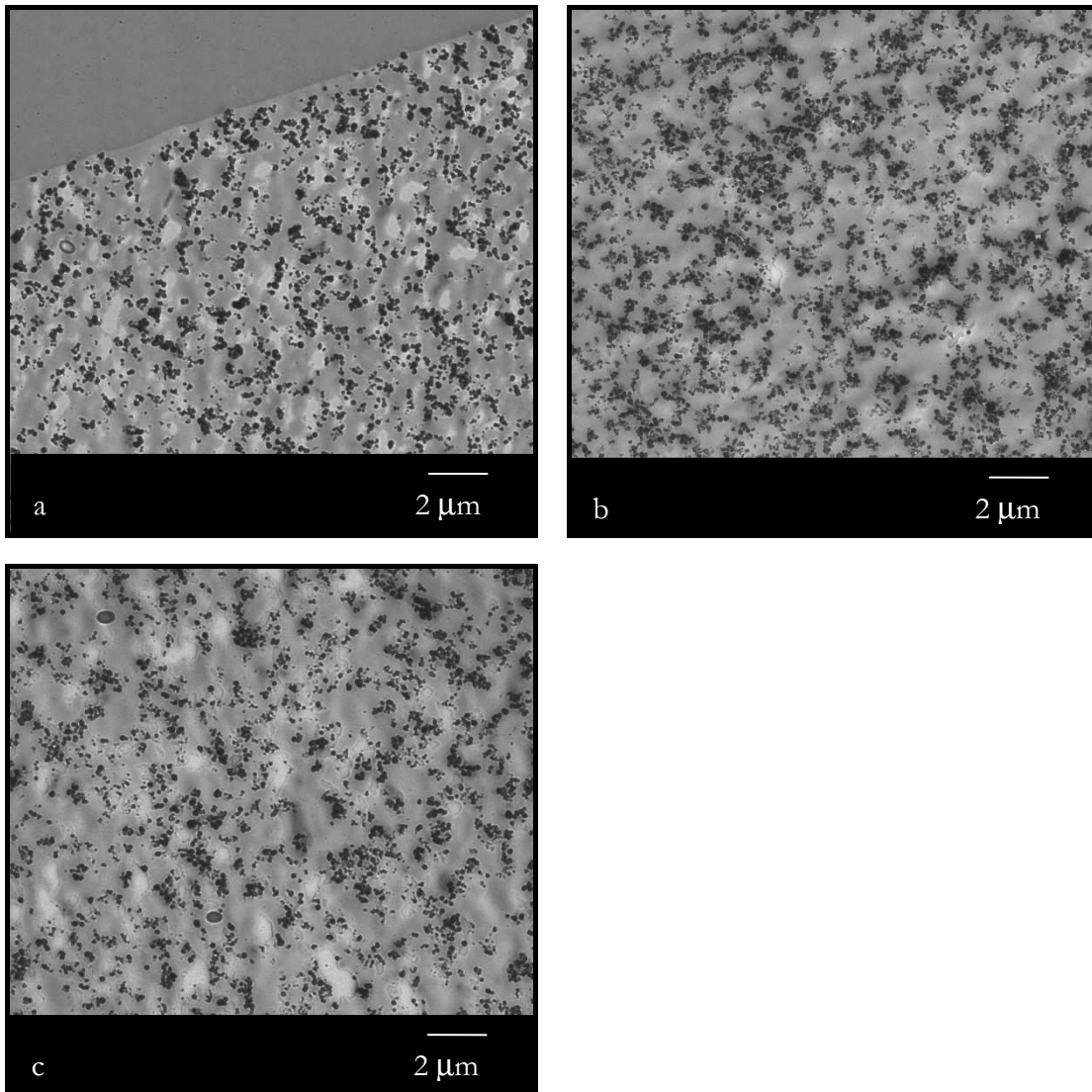


Figure 7: TEM of DP1100 reinforced with (a) 10 vol% of OX50 and (b) the same amount of APTMS surface modified OX50 and (c) GPTMS surface modified OX50

Transmission electron microscopy of coating samples reinforced with 10 vol.% unmodified silica nanoparticles show agglomeration of particles (Figure 7). These agglomerates, about 1-2 μm in size, are distributed uniformly throughout the coating cross section. Dispersion of nanoparticles was slightly improved by prior surface modification using amino- and glycidoxy silanes.

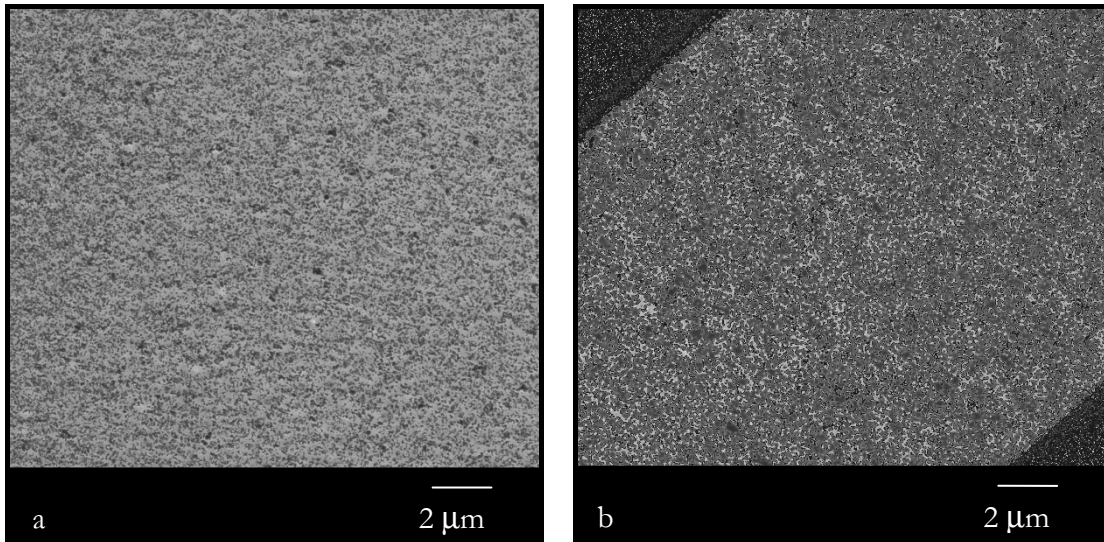


Figure 8: TEM of DP1100 reinforced with (a) 6 vol.% of AluC and (b) the same amount of APTMS-surface modified AluC.

Alumina nanoparticles are dispersed more uniformly in the polymer matrix than silica particles. There is also an even distribution of nanoparticles throughout the cross section. These findings apply to both non modified and surface modified nanoparticles as shown in Figure 8.

The transmission of UV and visible light is shown in Figure 9. For better comprehension only 5 samples showing best transmission performance are depicted. With increasing particle load the transmission performance deteriorates which becomes evident by comparison of curves 1, 2 and 5 in Figure 9 representing filling degrees of 6 vol.%, 10 vol.% and 20 vol.%, respectively, of the same coating composition. The coating composition containing 6 vol.% MPTMS surface modified silica nanoparticles shows best transmission behavior followed by 10 vol.% of the same composition.

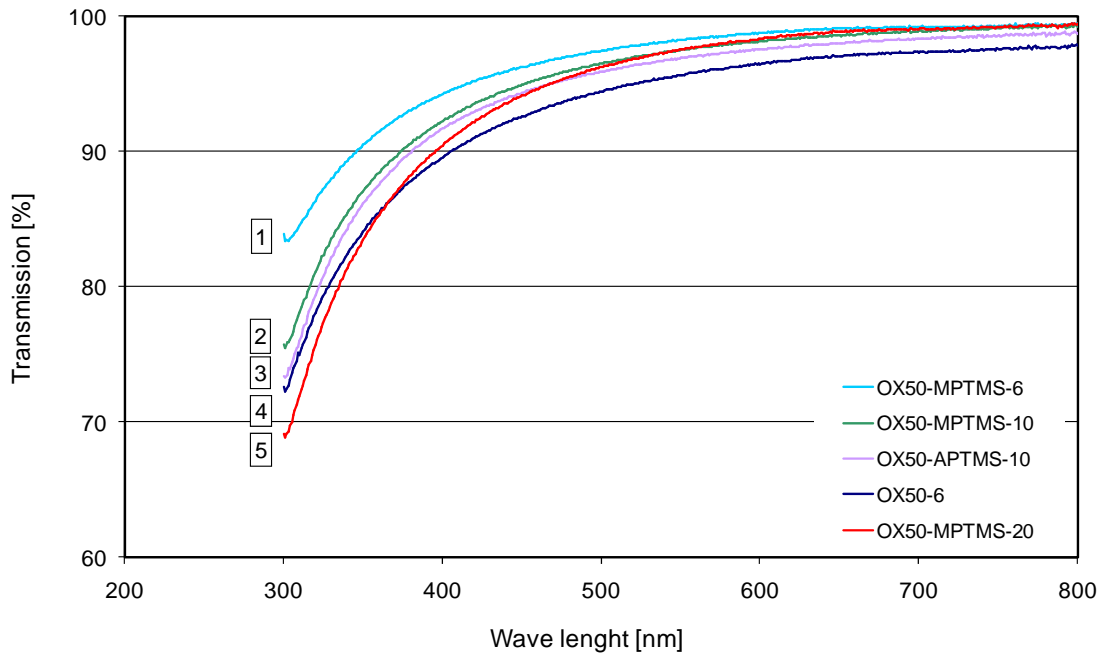


Figure 9: Transmission of 5 coating films showing best transmission performance.

6.4. Discussion

6.4.1. Mechanical and thermal properties

The improvement of the critical load was achieved for all nanoparticle filled systems. The polar nature of polyurethane components enabled good particle dispersion of the oxidic nanoparticles in the coating even without surface modification.

Although dispersion quality is similar for all compositions shown in Figure 7, values for critical load differ significantly. Composition OX50-PTMS-10 (Fig. 5b) shows hardly any improvement of critical load compared with the unfilled polyurethane. This might be due to the non reactive surface modification with propyltrimethoxy silane that cannot chemically react with the polymer matrix and hence does not actively reinforce the polyurethane network. Also results for residual depth back up this explanation. Composition OX50-GPTMS-10 (Fig. 5c) shows similar dispersion quality but achieved highest results for the critical load among compositions filled with 10 vol.% silica nanoparticles. We assume that particles with reactive end groups (APTMS, MPTMS and GPTMS) are chemically linked to the polymer network and hence lead to an increase in cross linking of the matrix. These findings are supported by DSC

6 Scratch behavior

measurements. Samples with high critical load values also show an increase in the glass transition temperature which also indicates an increase in cross linking.

These findings do not apply to the same degree for the alumina filled coatings. Here the good results of non modified alumina particles were only marginally improved by the surface modification with glycidoxypropylsilane (GPTMS). This effect might also be due to worse quality of the surface modification that was shown earlier for these alumina particles [8] and hence less available reaction sites on the particle surface.

Surprisingly, non modified silica and alumina particles show high reinforcement at very low filler loading of 6 vol.%. This indicates the possibility of a reaction between isocyanate hardener and OH groups on the particle surface. Additionally, a strong affinity between the nanoparticle surface and the polymer matrix can be assumed due to high polarity of both, particles and polymer. The formation of a layer of “bound polymer” on the nanoparticle surface that shows less mobility of polymer chains and leads to reinforcement is suggested. Because of higher surface area by a factor of 2 this effect is more pronounced for alumina filled compositions. As shown in Figure 4 and 3, T_g rises significantly by incorporation of 6 vol.% nanoparticles and decreases with the further increase of filler loading to 10 and 20 vol.%, respectively. We assume that agglomeration of particles takes place for higher filler loadings and thus less particle surface is available for interaction with the polymer matrix.

6.4.2. Optical properties

Transmission performance of coating films change for the worse with increasing volume fraction of silica and alumina nanoparticles. But still a considerable number of samples show more than 90 % transmission in the range of visible light. By comparison of samples OX50-6 and OX50-MPTMS-6 it can be assumed that organosilane layer reduces light scattering on the interface between the particle and the polymer matrix.

6.5. Conclusion

Clear coatings reinforced with non modified and organosilane grafted nanoparticles were prepared and characterised by means of mechanical and optical properties. A uniform dispersion of alumina particles throughout the cross section was achieved as shown by electron microscopy. Agglomeration was found in the case of silica filled compositions but these agglomerates were evenly distributed throughout the polyurethane films.

Nanoparticle filled polyurethane coatings showed considerable increase of the critical load achieved in Nano Scratch Tests in particular at low filler loadings. Furthermore the positive influence of organosilane surface modification featuring reactive end groups on the scratch behavior was shown. This indicates that surface modification with organosilanes featuring reactive end groups that can be chemically linked to the polyurethane network is favourable for scratch behavior.

However, good results of non modified nanoparticles lead to the conclusion that isocyanate hardener reacts directly with OH-groups on the particle surface and this also results in considerable mechanical reinforcement. Because of their easy processing and the absence of a surface modification step these compositions have high potential in industrial application.

Acknowledgements

We thank Mrs. Beatrice Fischer for collecting the DSC data and Nicolas Conté from CSM Instruments for providing the NST testing equipment. Financial support by CTI (commission for technology and innovation, Switzerland) is kindly acknowledged (project KTI 7351.2).

References

- [1] C. Zilg, R. Mülhaupt, J. Finter, *Macromol. Chem. Physic.* 1999, 200, 661.
- [2] B. Wetzl, F. Haupt, M. Qiu Zhang, *Compos. Sci. Technol.* 2003, 63, 2055.
- [3] V. Khrenov, M. Klapper, M. Koch, K. Müllen, *Macromol. Chem. Physic.* 2005, 206, 95.

6 Scratch behavior

- [4] F. Bauer, H.-J. Glasel, U. Decker, H. Ernst, A. Freyer, E. Hartmann, V. Sauerland, R. Mehnert, *Prog. Org. Coat.* 2003, 47, 147.
- [5] E. Barna, B. Bommer, J. Kursteiner, A. Vital, O. v. Trzebiatowski, W. Koch, B. Schmid, T. Graule, *Compos. Part A-Appl. S.* 2005, 36, 473.
- [6] D. Zhang, X. Jiang, C. Yang, *J. Appl. Polym. Sci.* 2003, 89, 3587.
- [7] in Degussa AG, *Schriftenreihe Pigmente*, Degussa AG, Frankfurt 1988.
- [8] E. Barna, D. Rentsch, B. Bommer, A. Vital, O. von Trzebiatowski, T. Graule, *KGK-Kaut. Gummi Kunst.* 2007, 60, 49.

7

Efficiency of commercially available silica organosols in the improvement of scratch resistance of polyurethane clear coatings^{*}

Abstract

The reinforcement of transparent polymer systems such as clear coating applications is a relatively new field of research. Nanoparticles allow for reinforcement of the mechanical properties of the polymer matrix without deterioration of transparency. When well dispersed in the polymer matrix there is only minor light scattering due to their size smaller than 100 nm. Unfortunately, nanoparticles tend to form agglomerates because of interparticle van der Waals forces. These agglomerates easily reach sizes of several hundred nanometers and cause an increased turbidity of the nanocomposite. In this work commercially silica organosols are incorporated in two polyurethane clear coating formulations. The morphology of particles and the dispersion quality in the coating films are investigated using transmission electron microscopy (TEM). The transparency of the nanocomposite films is measured by UV/vis spectroscopy. The effect of nanoparticle reinforcement on the mechanical properties is characterized by Dynamic Mechanical Thermo Analysis (DMTA) and the scratch resistance assessed by Nano Scratch Testing (NST).

^{*} E. Barna, A. Mielke, T. Graule, W. P. Meier, *to be submitted*.

7.1 Introduction

The dispersion quality of nanoparticles in a solvent which is then used for the coating system is a crucial step in the nanocomposite preparation as particles already agglomerated in the solvent can hardly be dispersed in the polymer matrix. In this work already dispersed commercially available colloidal silicas are used. A variety of aqueous based colloidal silicas is available on the market but only few solvent based systems that are appropriate for the polyurethane polymer matrix used in this study. Colloidal silica based on organic solvents is commonly called silica organosol.

7.2 Materials and Methods

Three types of Desmophen polyester polyol binder served as polymer matrix and were cured with stoichiometric amounts of Desmodur N3300 hardener. Desmophen types and Desmodur were purchased from Bayer MaterialScience, Germany. Dibutyltin dilaurate was used as a catalyst. Details of the coating components are given in Table 1. The properties of the three silica organosols are given in Table 2. Technical grades of methyl isobutyl ketone (MIBK) and n-butyl acetate (BuAc) were used as solvents.

Table 1: Properties of the polyester polyol binders and isocyanate hardener

Name	Function	Structure	Functional group [wt.%]	
Desmophen 800	binder	highly branched	OH	8.6 ± 0.3
Desmophen 1100	binder	branched	OH	6.5 ± 0.5
Desmodur N3300	hardener	HDI-Trimer	NCO	21.8 ± 0.3

All nanocomposite coatings were prepared by mixing the organosol and polyester polyol binder and adding the catalyst. Then a stoichiometric amount of hardener was mixed with this formulation and films applied to glass sheets using a doctor blade coater. The films were cured at 80 °C for 12 hours. Of each organosol films containing 4, 6 and 10 vol.% nanoparticles, respectively, were prepared for both types of coating. Also, a reference without nanoparticles was prepared of each coating formulation.

Nanoparticle size and morphology were determined by TEM. A drop of organosol was applied on a TEM copper grid and dried. Such prepared grids were investigated using a Philips CM 30 TEM. Cured coating films were characterised by Nano Scratch Testing (NST, CSM Instruments SA, Switzerland) to assess scratch resistance of the prepared nanocomposites. The scratch tests were performed under progressive load starting at 10 mN and increasing by 20 mN/min. The testing speed was 10 mm/min

for all tests. A Rockwell diamond indenter was used having a tip radius of 5 μm . After scratch testing the critical load, the force at which the coating starts to crack, was determined. Also the residual depth of the scratches was analysed. Dynamic Mechanical Thermal Analysis (DMTA) was performed on nanocomposite films using an ATM3 (Myrenne GmbH, Germany) in torsion mode at a testing frequency of 1.0 Hz with automatic data acquisition. Tests were carried out on rectangular samples of thickness between 0.22 and 0.33 mm in a temperature range between -100 and 150 $^{\circ}\text{C}$. Also, ultramicrotomed cross-sections of selected nanocomposite films were prepared to investigate the particle dispersion throughout the coating thickness using a Philips CM 30 TEM. Transparency of nanocomposite films was determined by transmission measurements using a Varian UV/vis spectrophotometer.

Table 2: Properties of silica organosols

Name	Producer	Primary particle size [nm]	SiO ₂ loading [wt.%]	solvent base	pH [-]
Nanopol XP21	Hanse Chemie	20	50	BuAc	3.5
Nissan MIBK-ST	Nissan Chemicals	10-15	30.5	MIBK	4.0
Highlink NanO G	Clariant	25	45	MIBK	3.5

7.3 Results and Discussion

TEM investigations were performed on both particles in solution and on ultramicrotomed cross-sections of the nanocomposite films containing 10 vol.% silica particles in Desmophen 1100 (Figure 1 to Figure 3). The particle size is in the range given by the supplier. Anyway, as evident in Figure 1a to Figure 3a the particle size distribution for Nanopol XP and Nissan MIBK-ST seems to be monomodal whereas the particles in Highlink NanO G show a bimodal size distribution with 25 and 10 nm, respectively.

When incorporated in the coating film all three organosols show different dispersion behaviour as shown in the cross-sections pictured in Figure 1b Figure 3b. Highlink NanoG particles are strongly agglomerated and there are regions in the cross-section showing no particles at all. Also, there is no aggregation of particles to be found on the surface of the film shown in the right part of Figure 1b. Although particles are

also agglomerated in the case of Nanopol XP, there is a layer of particles on both surfaces, the one on the glass sheet and the free surface on top of the film. Still, there is a major part in the bulk of the coating film without any particle reinforcement while some regions are packed with particles. Figure 3b shows the TEM image of the cross-section of the Desmophen 1100 coating sample filled with 10 vol.% of Nissan MIBK-ST. Here, the particles are uniformly dispersed throughout the cross-section even though agglomerates in the range of 100 to 600 nm are formed. Also, there is the formation of particle monolayers noticeable on both surfaces of the coating film (surface on glass substrate shown in Figure 3b, surface on top of the coating film not shown here). These differences in dispersion behaviour might be due to the surface modification of particles or the stabilization of particles in the solvent. Also, Nanopol XP particles were delivered in n-butyl acetate and thus the high agglomeration in the coating film might be the result of incompatibility of the n-butyl acetate with the coating system. As we do not have information about the surface modification or stabilization of the specific organosols we assume that in the case of Nissan MIBK-ST particles the modification shows more affinity to the coating system and thus these particles are more uniformly dispersed.

Reinforcement in terms of scratch resistance is achieved when the critical load leading to a breakdown of the coating surface is increased and the residual depth remaining after the scratch is minimized. Figure 4 shows the critical loads (l_c) of the references for both coating systems and for formulations filled with different amounts of silica particles. Formulations with Desmophen 800 generally show higher critical loads than those of Desmophen 1100. Formulations with Nissan MIBK-ST and Nanopol XP achieve higher values for l_c than the ones reinforced with Highlink NanO G. Whereas a filler loading of 4 wt.% seems to be ideal for Nanopol XP and Highlink NanO G, for Nissan MIBK-ST a higher loading of 6 wt.% shows the best results in terms of critical load. The improvement of critical load could be achieved for all formulations of Desmophen 800 with all three types of organosols. However, for Desmophen 1100 there is only marginal increase in the case of 4 wt.% of Nanopol XP and 6 wt.% of Nissan MIBK-ST and a decrease of critical loads for all other formulations.

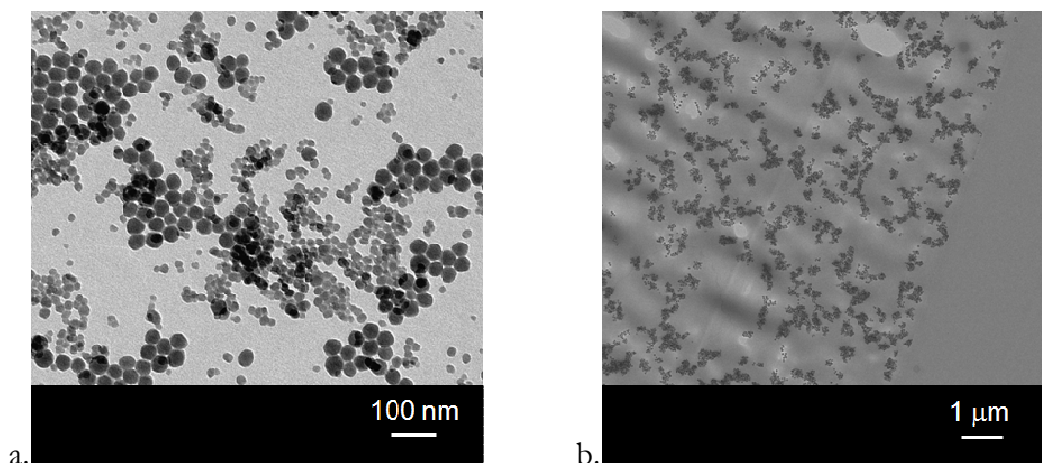


Figure 1: TEM images of Highlink NanOG particles (a) and 10 vol.% of these particles dispersed in Desmophen 1100 (b). The border shown in (b) represents the surface on top of the coating film.

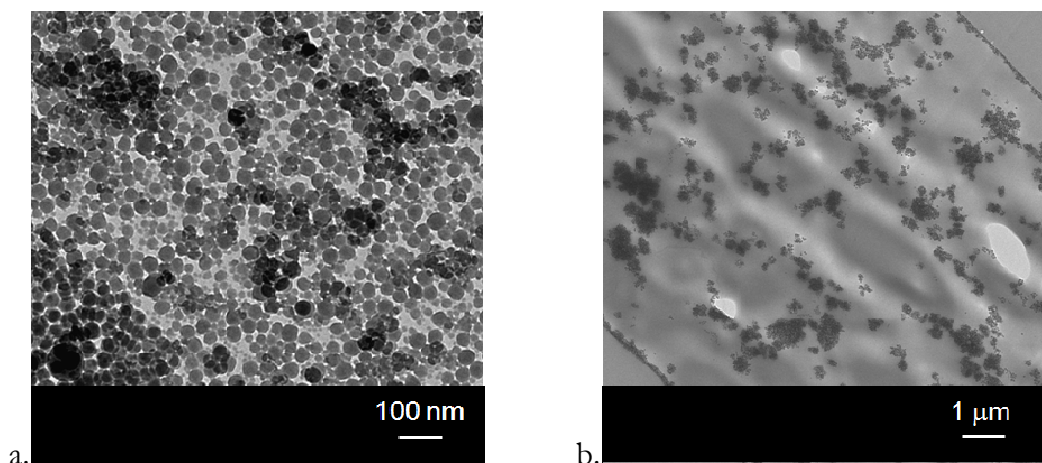


Figure 2: TEM images of Nanopol XP particles (a) and 10 vol.% of these particles dispersed in Desmophen 1100 (b). The border shown in the lower left part of (b) represents the surface on top of the coating film while the one in the upper right part is the surface on the glass substrate.

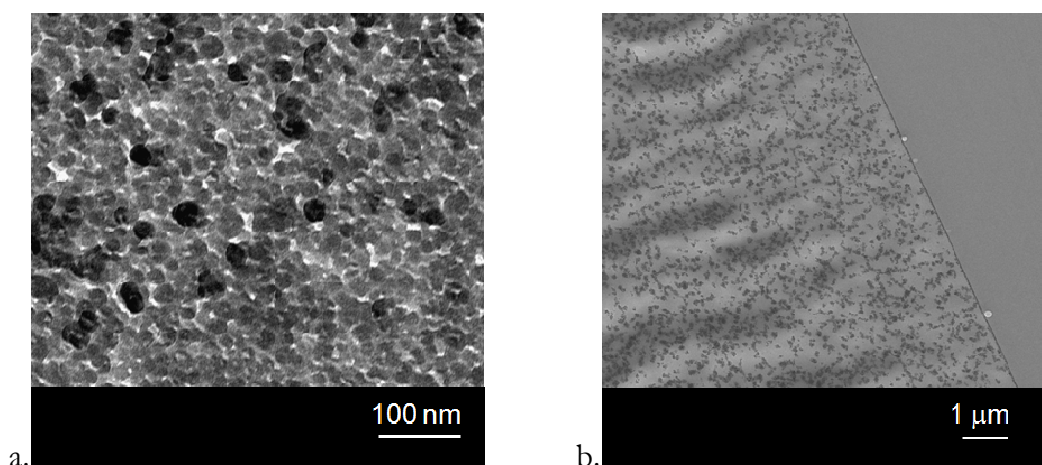


Figure 3: TEM images of Nissan MIBK particles (a) and 10 vol.% of these particles dispersed in Desmophen 1100 (b). The border in the right part of (b) represents the surface on the glass substrate.

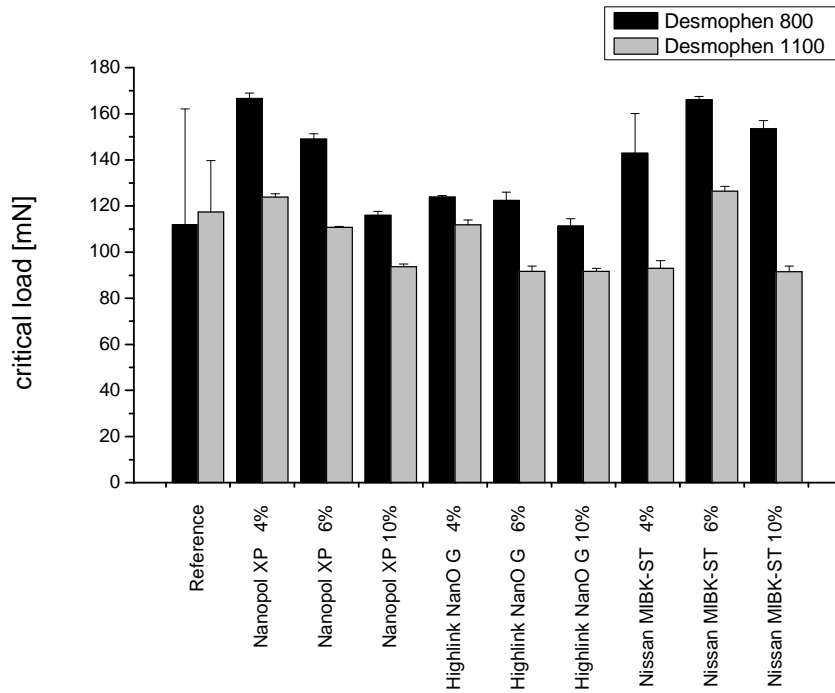


Figure 4: Critical loads of coating formulations reinforced with different amounts of silica particles.

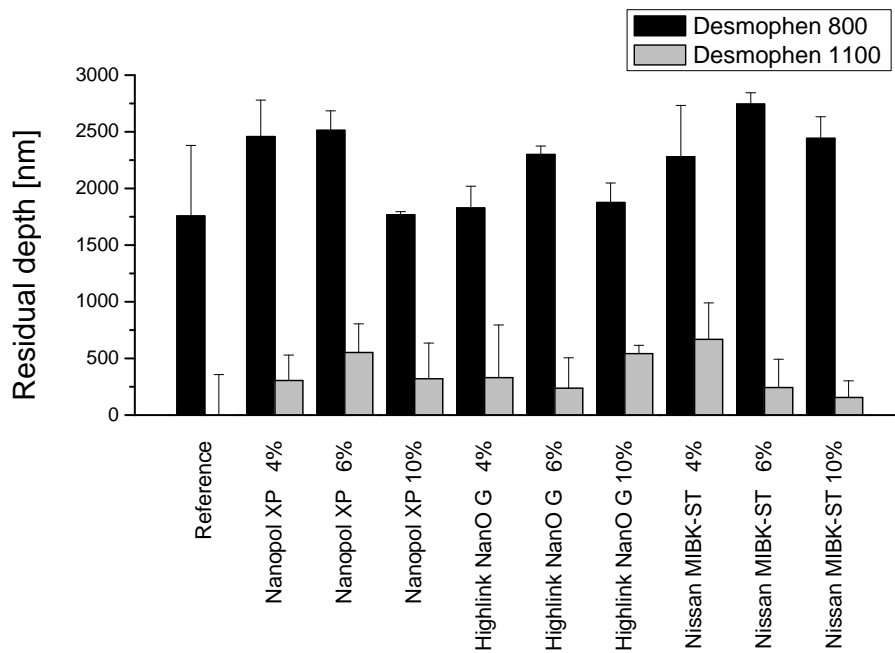


Figure 5: Residual depths of coating formulations with different amount of silica particles.

The residual depths (Rd) of scratches are depicted in Figure 5. The smaller the value for residual depth the more elastic is the deformation during scratching and the better the recovery of the coating after scratch deformation. A significant difference in behavior is apparent for the two coating systems Desmophen 800 and 1100. The unfilled reference of Desmophen 1100 shows no residual depth at all which implies a 100% recovery from scratching. That effect can be attributed to the different molecular structure of the polyester polyol base. Desmophen 800 is highly branched and has a higher number of reactive OH groups compared to Desmophen 1100. Therefore Desmophen 800 formulations have a higher degree of cross linking and in consequence less elasticity than the formulations with Desmophen 1100. All formulations reinforced with silica organosols show higher residual depths. This leads to the conclusion that an embrittlement of the coating takes place by the addition of silica particles. For Desmophen 800 formulations that results in easily detectable scratches of depths up to 2.7 μm . Due to the high elasticity of the unfilled Desmophen 1100 reference also filled formulations are relatively elastic leading to maximum depths of less than 1 μm which are acceptable because they are hard to detect by the naked eye in a possible future application. In addition to critical loads and residual depths also the appearance of the scratch path was qualitatively evaluated. The same trends in recovery behaviour of the two coating systems can be observed here. Figure 6 shows images of the two base coats Desmophen 800 and 1100 reinforced with the same amount of Nissan MIBK-ST particles. These images illustrate very well the findings described before. The Desmophen 800 coating basis shows predominantly plastic deformation while in Desmophen 1100 the elastic component prevails. Also visible in both images of Figure 6 are the cracks formed in the scratch path. The critical load was defined as the load that causes the first cracks in the scratch path.

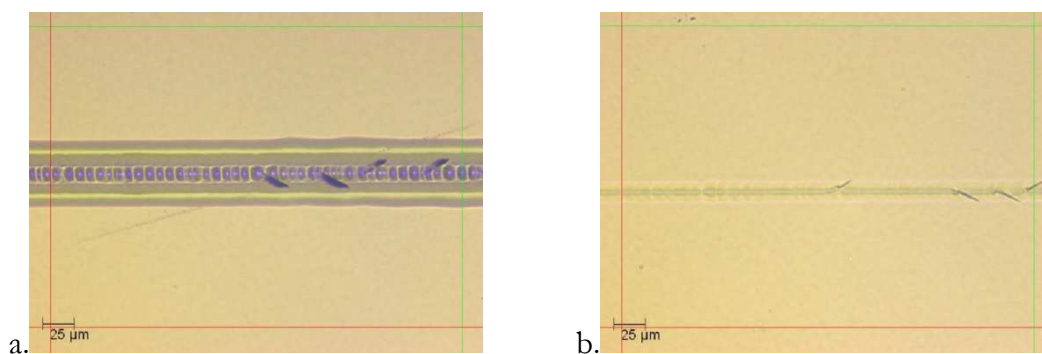


Figure 6: Images of the scratch path for a Desmophen 800 formulation containing 6 vol.% Nissan MIBK-ST particles (a) and the same formulation based on Desmophen 1100 (b).

The results of Dynamic Mechanical Thermal Analysis (DMTA) are shown in Figure 7 and Figure 10. Values for the glass transition temperature T_g are given in Table 1. Due to poor reinforcement results of Nanopol XP particles in the Scratch Testing and time restrictions these formulations were not included in the DMTA testing. Also, unfilled reference samples could not be analysed because of warping of the coating films after removal from the mold probably because of residual intrinsic stress. Figure 7 - Figure 10 show the typical curves of the shear modulus (G') and $\tan \delta$ versus temperature. There is a shift to higher T_g noticeable with increasing filler loading for Nissan MIBK-ST particles in both coating systems (Figure 7 and Figure 8). That correlation cannot be found for samples reinforced with Nanopol XP (Figure 9 and Figure 10). G' levels in the higher temperature range above the glass transition temperature allow for an estimation of the degree of cross linking of the test specimen. G' values are at a higher level for samples reinforced with Nissan MIBK-ST for both coating systems. Thus, the addition of Nissan MIBK-ST might lead to a higher degree of cross linking in the coating film. This correlates well with the findings from TEM investigations. Nissan MIBK-ST particles were uniformly dispersed throughout the cross section. Hence, these particles are well integrated in the polymer matrix and because of the minor agglomeration there is a maximum of particle surface in contact with the polymer matrix. In Figure 9 and Figure 10, showing the coating formulations with Nanopol XP, there is a second peak of $\tan \delta$ evident, in particular for the formulations containing 4 vol.% of silica particles. This peak formation indicates the existence of a second phase which might be a result of the insufficient dispersion of nanoparticles also shown in TEM images.

Table 3: Glass transition temperatures for silica reinforced coating formulations based on Desmophen 800 and 1100, respectively.

Sample		T_g [°C]	Sample		T_g [°C]
DP 800	4% Nissan MIBK-ST	35.6	DP 800	4% Nanopol XP	39.7
DP 800	6% Nissan MIBK-ST	43.3	DP 800	6% Nanopol XP	31.4
DP 800	10% Nissan MIBK-ST	43.6	DP 800	10% Nanopol XP	31.8
DP 1100	4% Nissan MIBK-ST	15.6	DP 1100	4% Nanopol XP	19.4
DP 1100	6% Nissan MIBK-ST	19.4	DP 1100	6% Nanopol XP	15.3
DP 1100	10% Nissan MIBK-ST	23.6	DP 1100	10% Nanopol XP	19.7

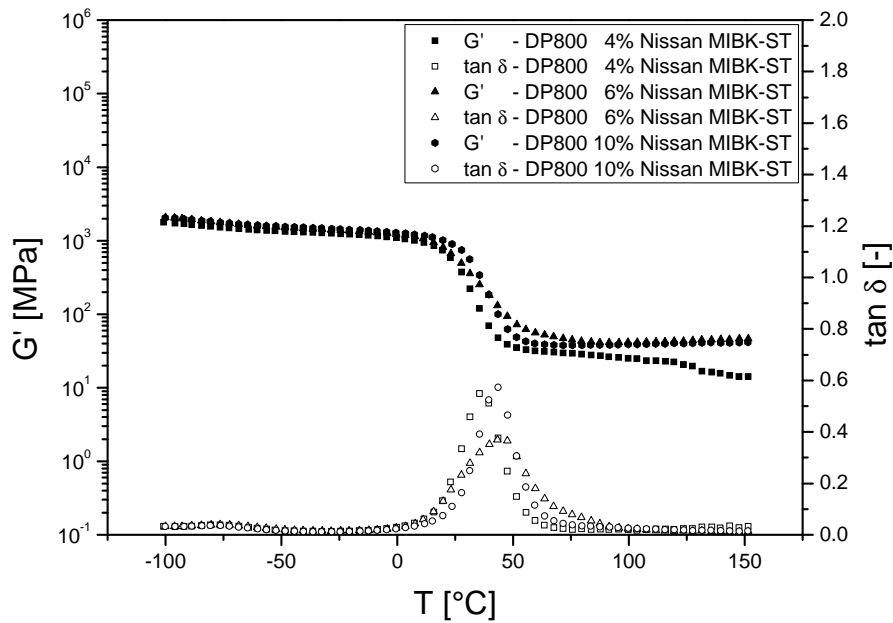


Figure 7: Temperature dynamical mechanical behavior of Desmophen 800 coating formulations reinforced with different amounts of Nissan MIBK-ST silica particles.

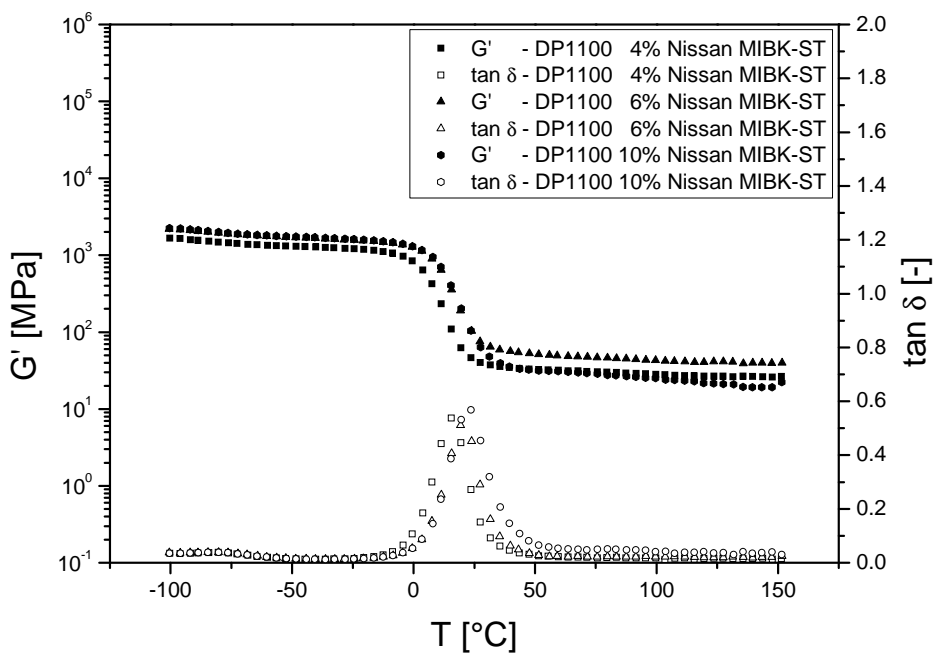


Figure 8: Temperature dynamical mechanical behavior of Desmophen 1100 coating formulations reinforced with different amounts of Nissan MIBK-ST silica particles.

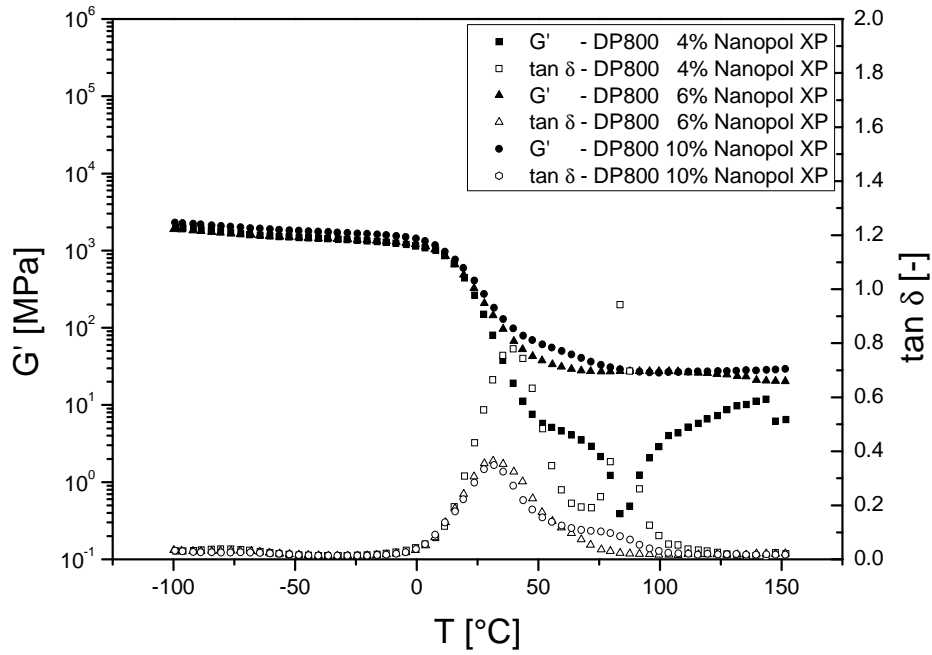


Figure 9: Temperature dynamical mechanical behavior of Desmophen 800 coating formulations reinforced with different amounts of Nanopol XP silica particles.

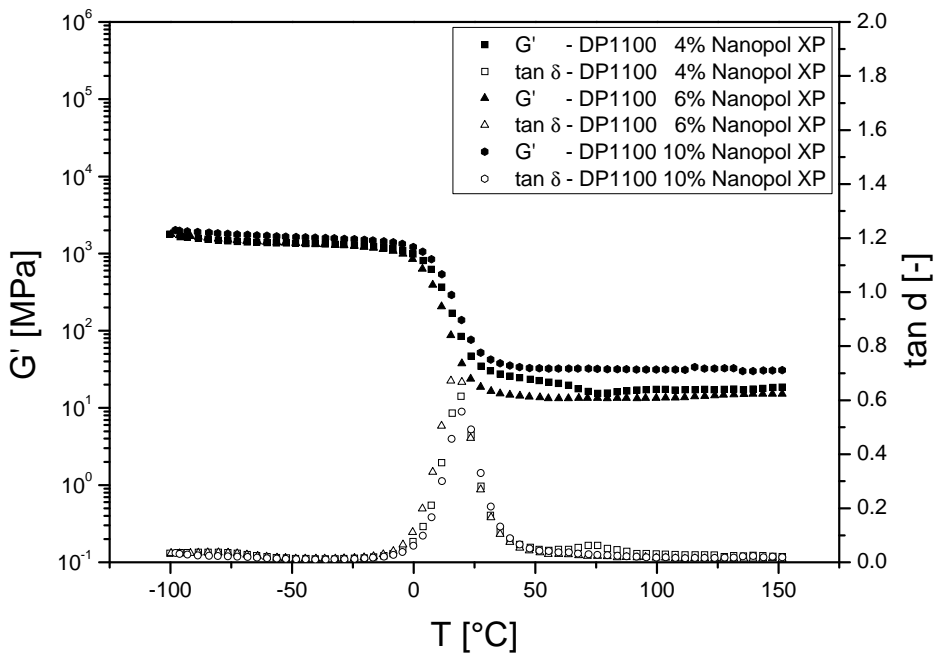
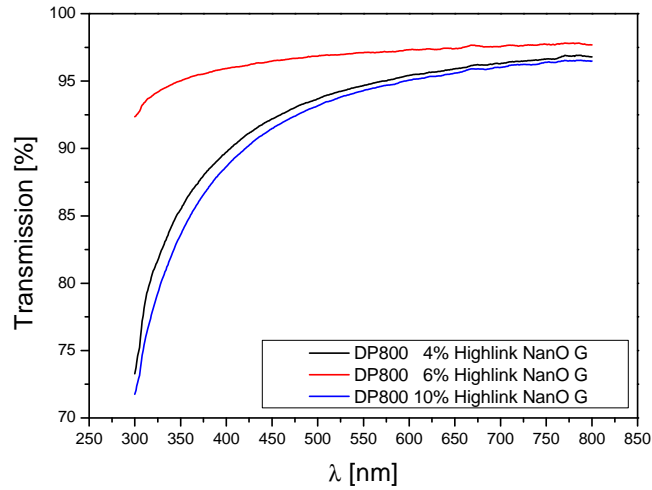


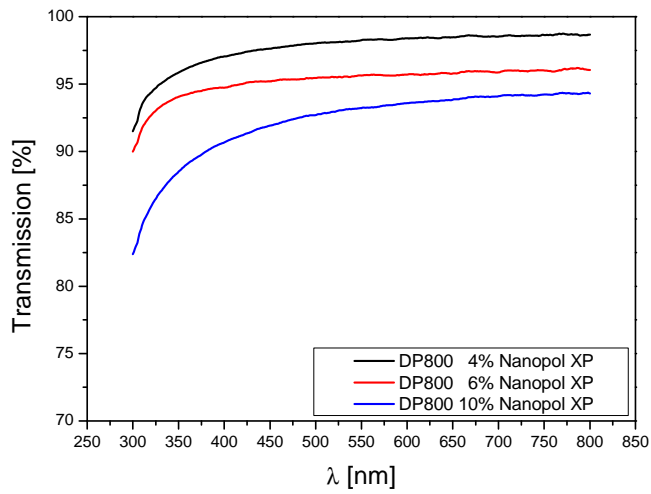
Figure 10: Temperature dynamical mechanical behavior of Desmophen 1100 coating formulations reinforced with different amounts of Nanopol XP silica particles.

The transparency of a clear coating formulation can be determined by accessing the transmission in the range of visible light. Also, information is gained on the dispersion quality of the filled coating systems. The unfilled coating samples were measured first and then set as the 100 % value. The transmission of Desmophen 800, comprising 4, 6 and 10 % of the three organosols used in this work is shown in Figure 11. For the samples filled with Highlink Nano G there is a good transmission performance for formulations with 6 % silica particles but for 4 % and 10 %, respectively, transmission is quite low. Starting at 70 % transmission for shorter wavelengths the transmission values do not exceed 95 %. However, the 6 % formulation shows values between 91 for short wavelengths and 97 % for long wavelengths. As seen before in TEM images for Highlink NanO G, particles tend to agglomerate and phase separate. Thus, results for 4 and 6 % filling rate are more realistic and it has to be assumed that the measurement was carried out in a region having less agglomerations of particles. In the case of Nanopol XP (Figure 11a) there is a decrease in transmission evident with increasing filler content. Best transmission results were achieved with formulations containing Nissan MIBK-ST nanoparticles. Results for all three filling rates are in the same region between 92 and almost 100 %. That correlates well with the findings of TEM images where Nissan MIBK-ST nanoparticles were uniformly dispersed. Thus, minor interaction with incident light has to be assumed and can be accounted for high transmission values.

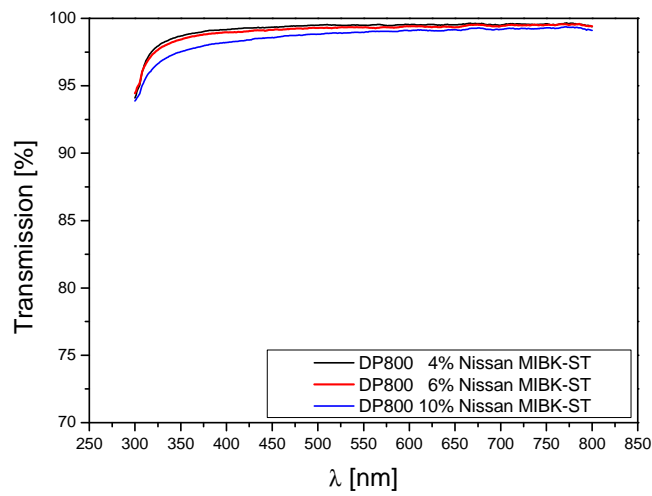
In general formulations based on Desmophen 1100 are more transparent than those of Desmophen 800. All formulations containing Highlink NanO G and Nanopol XP show higher transmission than samples with the same filler content but based on Desmophen 800. Values are in the range between 93 and almost 100 % transmission. Also transmission for Nissan MIBK-ST particles is improved but here the poor transmission for the sample reinforced with 4 % nanoparticles is surprising. No such behavior was noticed for the same sample based on Desmophen 800. Improvements in transmission may be due to lower viscosity of the Desmophen 1100 binder and thus better miscibility with the different organosols.



a.

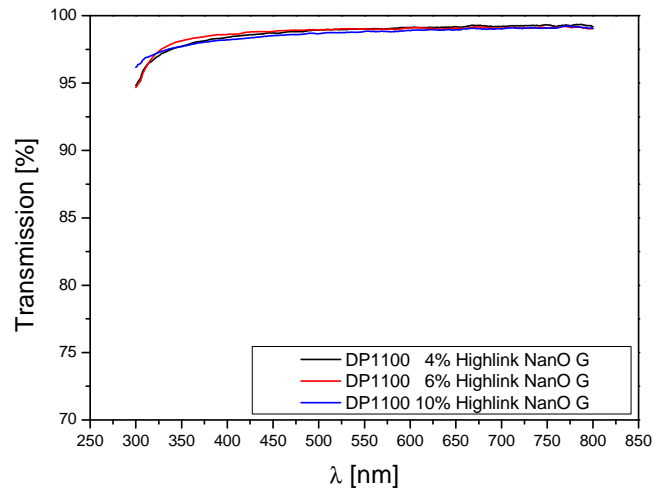


b.

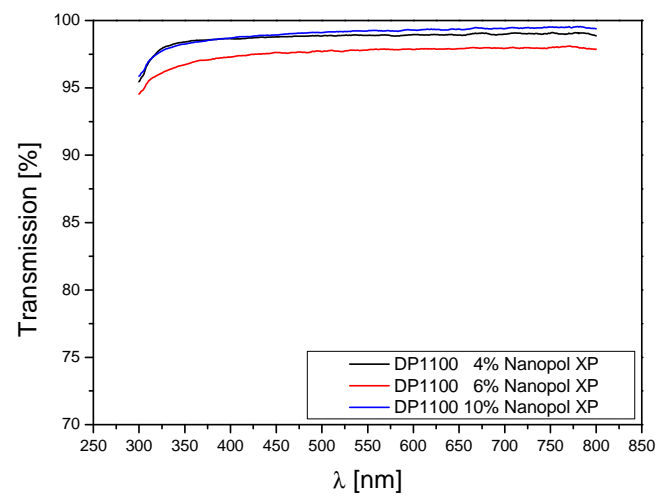


c.

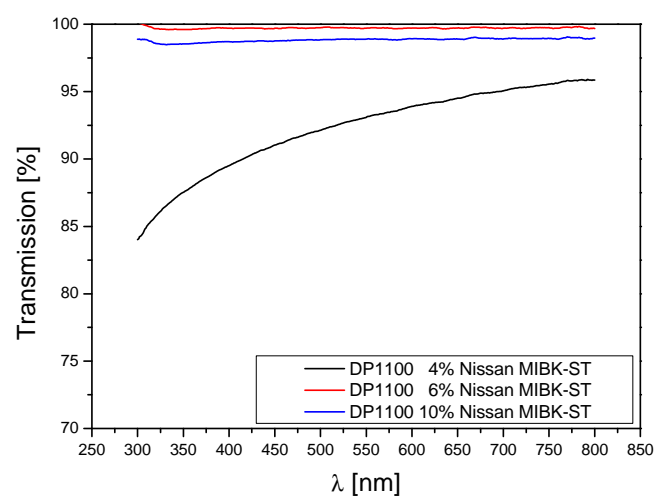
Figure 11: Transmission of Desmophen 800 coating formulations reinforced with different amounts of fillers.



a.



b.



c.

Figure 12: Transmission of Desmophen 1100 coating formulations reinforced with different amounts of fillers.

7.4 Conclusion

In this work three different kinds of organosols were incorporated in two polyurethane clear coat formulations in order to improve scratch resistance without deterioration of optical transparency.

For the coating system based on Desmophen 800 the improvement of scratch properties in terms of critical load was achieved for all formulations. Best results are obtained with formulations reinforced with 4 % Nanopol XP and 6 % Nissan MIBK-ST, respectively. Also, the residual depth of scratches is increased indicating an unwanted embrittlement of the nanocomposite compared to the unfilled coating. The transmission measurements show excellent transparency for the formulation of 6 % Nissan MIBK-ST in Desmophen 800.

The formulations based on Desmophen 1100 show different mechanical behaviour. The increase of critical load by nanoparticle addition is not as pronounced as in Desmophen 800 formulations but there is also less embrittlement caused by the silica organosols and thus residual depths are in a tolerable range. For these formulations best results are achieved with a concentration of 4 % Nanopol XP particles. The transparency for all formulations is exceeding than 95 %.

8

Refractive index matching of silica/alumina mixed oxide nanoparticles for scratch resistant clear coatings*

Abstract

A new route to transparent polymer nanocomposites is reported. Specifications for such composites are conflicting as nanoparticles have to be as small as possible to avoid light scattering and thus turbidity of the coating film. But the smaller the particles the more difficult good dispersion quality can be achieved because interparticle van der Waals forces increase which finally lead to agglomeration. In this work we produced tailor made mixed oxide nanoparticles of various $\text{SiO}_2/\text{Al}_2\text{O}_3$ compositions by Flame Spray Synthesis. Thus it is possible to match the refractive index (RI) of nanoparticles to the coating film. As a result the Hamaker constant of the system is reduced leading to a decrease of van der Waals attractive forces between nanoparticles. That way nanoparticle dispersion in the polymer is enhanced and higher transparency achieved. Nanoparticles are characterized by BET, TEM and XRD. Nanocomposite coatings are prepared and UV-vis measurements carried out to determine transparency. Furthermore coating samples are ultramicrotomed and cross sections investigated by TEM to allow statements on dispersion quality. Coating films filled with refractive index matched particles show significantly higher transmission and thus higher transparency than coatings filled with non-matched particles.

* E. Barna, A. Vital, C. Weiher, W. P. Meier, T. Graule, *submitted to Advanced Functional Materials*.

8.1. Introduction

Reinforcing polymers with the help of inorganic nanoscale particles has opened a wide field of properties that was inaccessible by conventional fillers.^[1-5] Polymer properties such as tensile strength, wear and scratch resistance can be improved without deterioration of optical properties and embrittlement.^[6-9] Nanoscale fillers are particularly interesting in transparent applications such as clear coating systems. In order not to interact with incident light and thus cause a reduction of transparency either the particle size of the filler has to be in the lower nanometer range and/or the refractive index of the particles has to match that of the polymer matrix. Due to a rise of interparticle van der Waals forces occurring with decreasing particle size, nanopowders are typically hard to disperse in non polar solvents and thus often used as additives to adjust rheology ^[10, 11]. Hence in particular very small particles tend to form agglomerates that cause scattering of visible light and turbidity of the cured coating.

Scattering of light on small particles is described by the Rayleigh equation:

$$\frac{I_s}{I_0} = \frac{(1 + \cos^2 \theta)}{2R^2} \left(\frac{2\pi}{\lambda} \right)^4 \left(\frac{\left(\frac{n_p}{n_M} \right)^2 - 1}{\left(\frac{n_p}{n_M} \right)^2 + 2} \right)^2 \left(\frac{d}{2} \right)^6 \quad (1)$$

where I_s is the intensity of scattered light and I_0 the one of incident light. R is the distance to the particle, θ is the scattering angle, λ is the wave length of unpolarized light, n_p is the refractive index of the filler particles and n_M the one of the polymer matrix and d is the diameter of the particle ^[12]. There are two possible ways to reduce scattering of light and thus loss of transparency: either n_p resembles n_M or the particle diameter is reduced.

A promising solution to improve the coating transparency is to match the refractive indices of filler particles (n_p) to that of the polymer matrix (n_M). Thus no scattering of light occurs on the filler surface and the coating remains transparent. An additional benefit of matching the refractive indices of filler particles and polymer matrix is the reduction of the Hamaker Constant and as a result the reduction of van der Waals attractive forces between particles. In consequence less agglomeration of nanoparticles in the polymer matrix can be expected. This effect is well known in colloid science but

to our knowledge has not been reported in the context of transparent polymer nanocomposites.

Commercially available two pack polyurethane clear coating systems typically have refractive indices of about 1.50. Based on theoretical considerations particles in that range can be produced by mixing silica with alumina, titania or zirconia in an adequate proportion. Experiments with titania and zirconia showed the existence of crystalline phases at the required mixing ratios. Only by mixing silica with alumina having refractive indices of 1.46 and 1.69, respectively, was it possible to produce continuously amorphous nanoparticles in the RI range in question. To obtain optimum transparency in the lacquer the refractive index throughout the particles has to be constant and thus the synthesized material has to be a homogeneously mixed oxide and not a nanocomposite of the two oxides used. Furthermore a spherical morphology is preferable because of a resulting low specific surface area which has a positive influence on the viscosity of the uncured coating composition.

Refractive indices (RI) of composite materials and in particular of glasses can be calculated using the equation

$$n = 1 + \rho \sum f_i^{HS} \cdot w_i \quad (2)$$

by Huggins and Sun.^[13] n is the refractive index of the composite, ρ is the density of the composite, w_i is the mass fraction of contents and f_i^{HS} is a material specific factor. ρ is calculated using the equation

$$\rho = \frac{1}{\sum d_i^{HS} \cdot w_i} \quad (3)$$

with d_i^{HS} being a second material specific factor. f_i^{HS} and d_i^{HS} can be found in literature.^[13]

Nanometer sized oxide particles are commonly synthesized by sol gel route, more specific the Stöber process.^[14] The advantage of this synthesis route is that high monodispersity can be achieved and resulting nanoparticles are non-agglomerated. In the case of mixed oxide particles this method has the major drawback that both precursors have to show similar reaction rates to form mixed oxide particles of a given composition.^[15] Flame spray synthesis is an alternative allowing the production of a variety of powders only limited by the miscibility of precursors.^[16] For the synthesis of

8 Refractive Index Matching

oxidic nanoparticles metal-organic precursors are diluted in solvents that are preferably but not necessarily flammable. The diluted precursors are then sprayed centrally into a flame where the solvent and precursor are burned and form oxidic particles. To produce mixed oxide nanopowders precursors of component A and B are mixed in the required mol-ratio and subsequently processed. As the precursor feed is operated with a syringe pump high flexibility concerning changing compositions is provided. Also long term experiments with regular sampling and determination of refractive indices showed high process stability.

8.2. Results and Discussion

8.2.1. Nanoparticle Synthesis and Characterization

Small amounts of mixed oxide nanoparticles with different molar ratios starting from pure silica up to pure alumina were prepared by Flame Spray Synthesis. These nanoparticles were characterized by XRD, BET nitrogen adsorption and TEM. In special refractive indices of particles and polyurethane coating were determined. Then nanoparticles in the refractive index range of the coating were produced in bigger quantities.

Specific surface area (SSA) of several compositions is shown in **Figure 1**. A decline in SSA which indicates an increase in particle size can be observed with higher alumina content. From 40 wt% on the specific surface area and hence particle size is largely stable at a value around 50 m²/g. That might be due to the different viscosities of used precursors for silica and alumina. Alumina precursor has a higher viscosity and because of constant production parameters compositions with higher Aluminum-sec-butoxide content form bigger droplets which result in bigger particles.

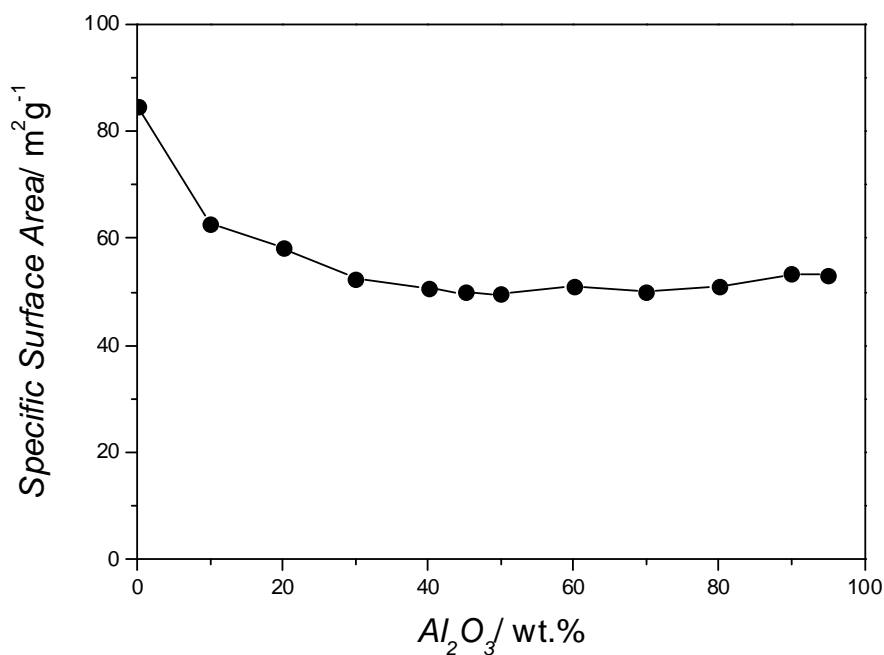


Figure 1. Specific surface area (SSA) of different compositions measured with BET method

Mixed oxide nanoparticles were also characterized by x-ray diffraction. Resulting spectra are shown in **Figure 2**. For low alumina contents XRD measurements show a persistent amorphous phase and the existence of a peak typical for amorphous silica which can be found in the range between 20 and 25 2θ . With the increase of alumina content this peak is shifted to higher theta values. That can be ascribed to Al atoms being build in the amorphous silica network and thus altering the long range order of silica. Starting from 60 wt% peaks appear in the XRD spectra that are related to crystalline γ -alumina phases. For higher alumina contents the miscibility of the systems might be reached and thus there is a phase of surplus alumina which forms phases that show crystalline order.

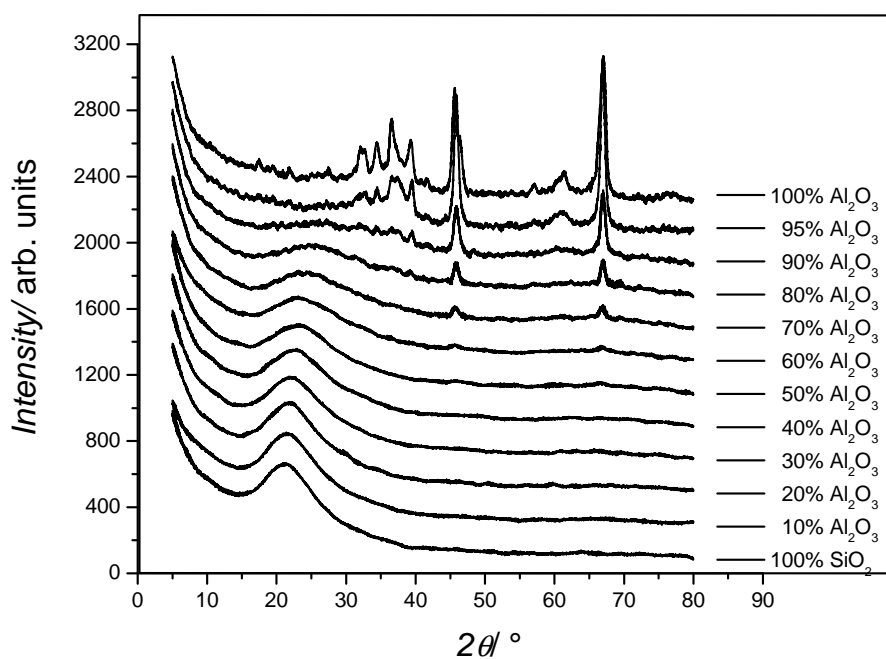


Figure 2. XRD curves of various $\text{SiO}_2/\text{Al}_2\text{O}_3$ compositions

Morphology of nanopowders was investigated by transmission electron microscopy (TEM). Nanoparticles shown in **Figure 3a** consist of 70 wt% silica and 30 wt% alumina and are of spherical shape. No crystalline pattern can be found for the composition shown in **Figure 3b** which also confirms the hypothesis of an amorphous silica/alumina mixed oxide phase for compositions with alumina contents smaller than 60 wt%.

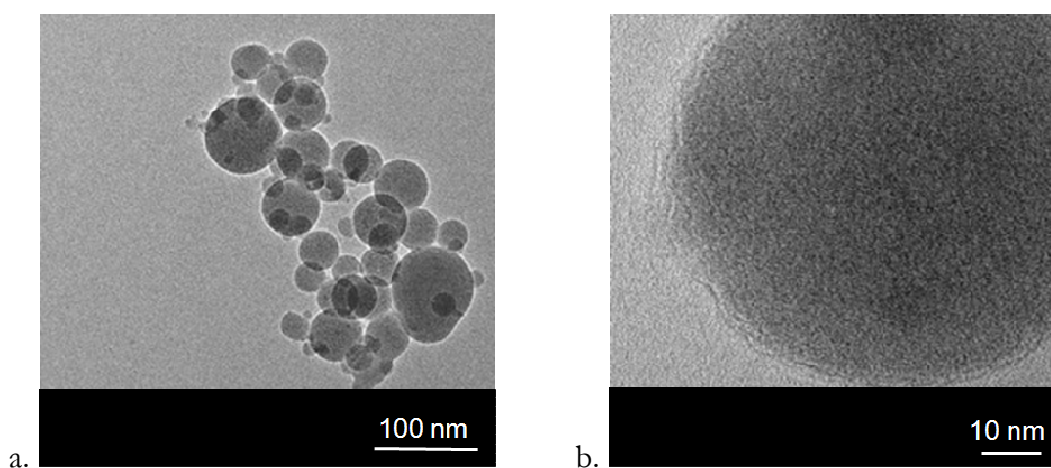


Figure 3. TEM images of mixed oxide nanoparticles containing 70 wt% SiO_2 and 30 wt% Al_2O_3

Calculations of refractive index have been done based on the empirical equation postulated by Huggins and Sun (**Equation 2**). This equation takes into account the density of the mixed oxide, a material specific factor and the mass fraction of the components. Refractive indices have been determined for all produced powders using the Becke Line Method. Pure SiO_2 has a refractive index of 1.460 and pure Al_2O_3 of 1.690, respectively. Results of both, calculation and measurement are depicted in **Figure 4**. The curve shows theoretical values and measured refractive indices are marked with points. RI of Desmophen 800 coating is represented by the horizontal dotted line. Up to 40 wt% alumina measured results are in good agreement with calculated values. For higher alumina content measured refractive indices are slightly lower than calculated ones. This might be due to the fact that the formula was originally elaborated for amorphous glasses. Also XRD measurements show the existence of a crystalline phase for compositions with alumina content of more than 50 wt%.

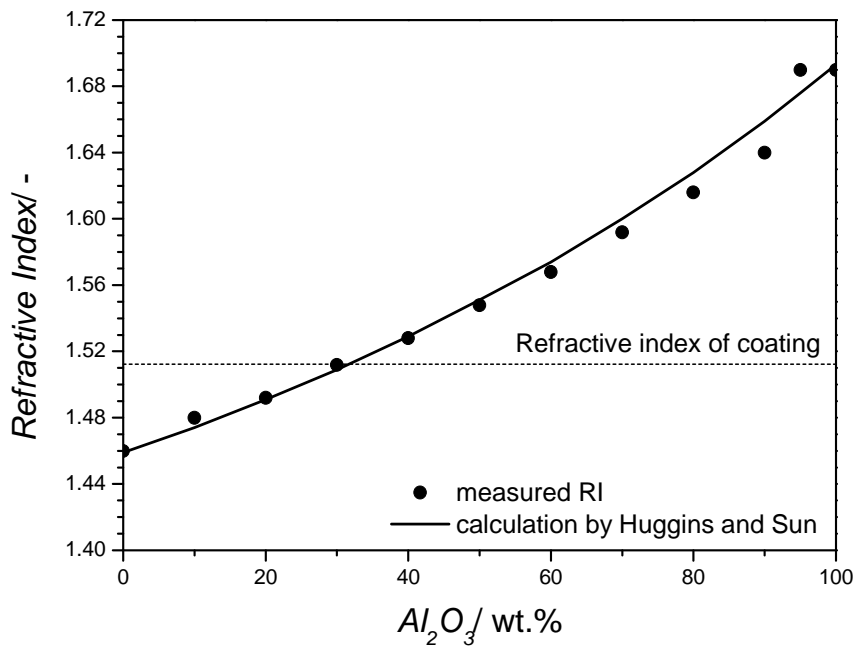


Figure 4. Measured RI (points) and theoretical RI (line) calculated according the equation by Huggins and Sun

8.2.2. Nanocomposite Coatings

The refractive index of our polymer system was measured to be 1.512 and according to Figure 4 nanoparticles consisting of 40 wt% alumina and 60 wt% silica are supposed to have the same RI.

Results of UV-vis measurements are shown in **Figure 5**. At a filler loading of 10 wt% the coating bearing the non-refractive index matched silica particles shows lowest relative transmission whereas mixed oxide particles with a refractive index matched to that of the coating system induce less scattering which results in a significantly higher relative transmission. Best results are obtained when RI matched particles (40 wt% alumina) are dispersed in the coating with the help of a dispersion additive. For coating compositions with 20 wt% particles incorporated results show the same tendency but are even more pronounced.

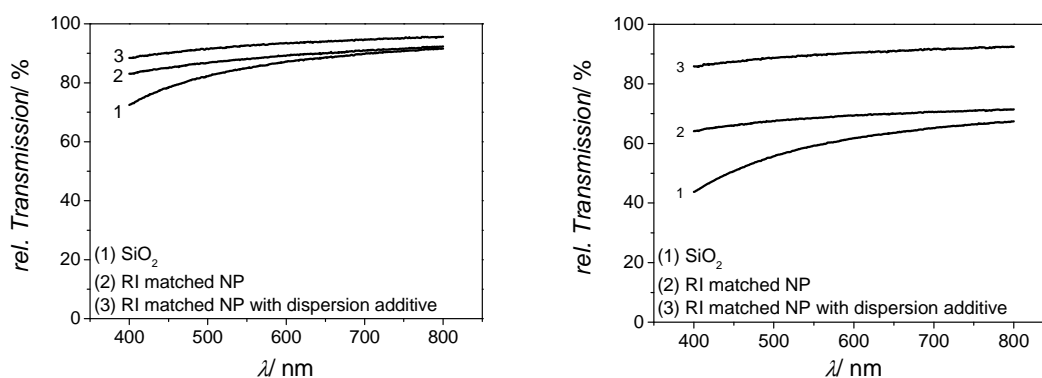


Figure 5. Relative transmission of coatings reinforced with 10 (left) and 20 wt% filler particles (right), respectively

TEM images of ultramicrotomed samples were taken of a coating filled with 20 wt% of mixed oxide nanoparticles of matched refractive index and with pure silica to investigate dispersion of nanoparticles throughout the coating layer. **Figure 6a** and **Figure 6b** show these cross sections. The coating reinforced with non matched nanoparticles shows large areas without particle (Figure 6a) whereas refractive index nanoparticles are considerably more uniformly dispersed in the coating with a lower tendency to aggregate.

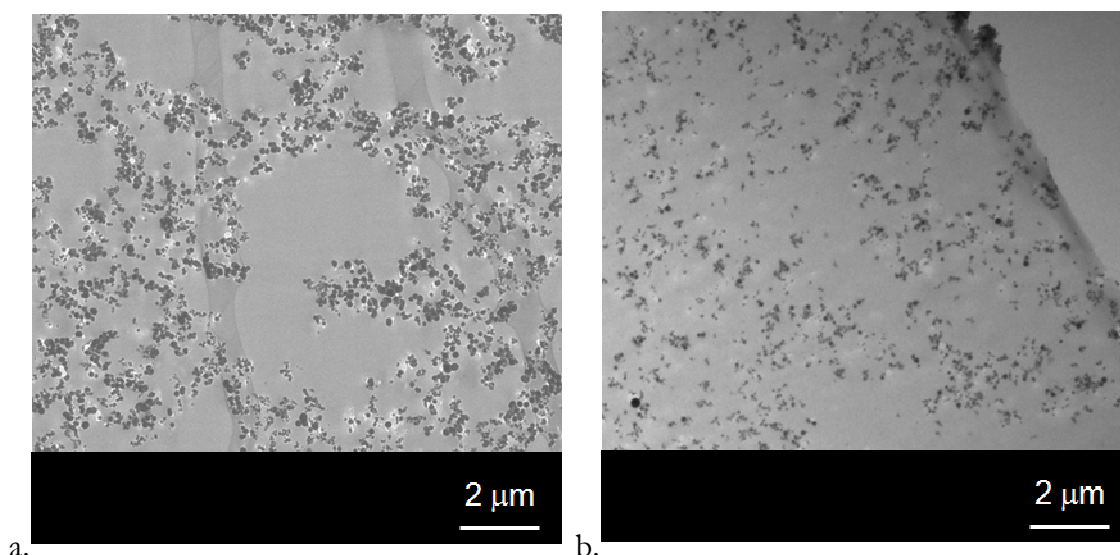


Figure 6. TEM image of ultramicrotomed coating samples filled with (a) 20 wt% SiO₂ nanoparticles and (b) the same amount of mixed oxide nanoparticles (40 wt% SiO₂/60 wt% Al₂O₃)

8.3. Conclusion

In this work the production of non aggregated spherical nanoparticles of silica-alumina mixed oxide via Flame Spray Synthesis was achieved. Furthermore the refractive index of the nanoparticles was influenced by the composition of precursors and was adjusted to match the refractive index of a commercially available coating system. Refractive index matched silica-alumina mixed oxides can be produced in the RI range between 1.42 and 1.55. The process of flame spray synthesis of mixed oxide nanopowders shows high reproducibility. Production rates of up to 100 g/h were realized with an RI accuracy of 0.002. Nanoparticles show amorphous behavior up to 50 wt% alumina. For higher alumina contents typical peaks for γ -alumina crystalline phases were observed in XRD measurements. In the amorphous range, up to 50 wt% alumina measured values for RI are in good agreement with values calculated with the equation by Huggins and Sun. Anyway, we achieved to produce tailor made nanoparticles with an adjustable refractive index in the range from 1.460 to 1.690, respectively. When RI-matched nanopowder is incorporated in a 2 component polyurethane clear coating system coating films reinforced with RI-matched nanoparticles showed significantly higher transmittance than coatings filled with the same amount of silica nanoparticles of comparable size. Thus a minimum of light scattering on the polymer/particle interface can be assumed and can be attributed to minimum differences in refractive index. It has to be emphasized that we successfully

8 Refractive Index Matching

incorporated 10 and 20 wt% of RI-matched nanoparticles in a transparent polyurethane coating film with only a minor loss of transparency. We take that as a confirmation of our initial hypothesis when we postulated a more uniform dispersion of refractive index matched nanoparticles due to a reduction of van der Waals forces going along with a reduction of the Hamaker constant of the system.

In a subsequent step these particles can be surface modified using silanes bearing end groups such as mercapto and amino groups which can be reactively linked to the polymer matrix [17-19]. Such modified fillers allow for the mechanical improvement of transparent coatings with only minor losses of optical performance.

8.4. Experimental

8.4.1. Flame Spray Synthesis

Nanoparticles in this study were prepared using a flame spray device designed and built at High Performance Laboratory at EMPA, Switzerland. The flame spray device consists of gas and liquid feed controllers, a spray burner and a powder collection unit. The burner is a block nozzle of a commercial flame cutter (Type 150-200, Pangas, Switzerland) with a 3 mm outlet diameter and six pre-heating flames (outlet diameter 1 mm) surrounding the centre gas outlet at a distance of 1.5 mm. A capillary tube (1.6 mm outer diameter, 1.05 mm inner diameter) was placed concentrically in the centre gas outlet and the tube outlet was leveled with the burner mouth to form an external mixing nozzle. The flow rate of the precursor solution was controlled volumetrically via a continuous double syringe pump (PN1610, Postnova, Germany) to the capillary tube and atomized at the exit by the oxygen (99.95 %, Carbagas, Switzerland) supplied through the centre gas outlet. Oxygen and acetylene (both >99.5 %, Carbagas, Switzerland) for the carrier flames were pre-mixed in the block nozzle with a flow rate of 12 l/min and kept constant in all experiment series. All gas flow rates were metered by mass flow controllers (MFC, Bronkhorst, Netherlands). The powder produced was collected in a baghouse filter (Friedli AG, Switzerland) and representative powder samples (0.5 to 1 g) were simultaneously deposited on a glass fibre filter (ϕ 150 mm; Schleicher-Schüll, Germany) by means of a vacuum pump (VCA 25, Rietschle-Thomas, Switzerland). To produce silica/alumina mixed oxide nanoparticles of a certain composition precursors A and B, in this study

hexamethylenedisiloxane and aluminium sec.-butoxide, respectively, are mixed in the required mol-ratio and subsequently processed.

8.4.2. Particle Characterization

The specific surface area (SSA) of the flame synthesized powders was determined by a five-point N₂ adsorption isotherm applying the BET (Brunauer-Emmett-Teller) method (Beckman-Coulter SA3100). Prior to measurement the powder samples were degassed for three hours at 200 °C under flowing nitrogen to remove adsorbed water from the particle surface. From the specific surface area the BET-equivalent particle diameter d_{BET} (Sauter diameter) can be back-calculated assuming monomodal and spherical particles.

X-ray diffraction (XRD) was used to determine the phase composition of the powders. The analysis was performed with a Siemens D500 instrument. Diffraction patterns were recorded from 20° to 80° 2 θ angles using Ni-filtered CuK α radiation.

Analysis of the particle morphology was performed by means of a transmission electron microscope (TEM) (Philips CM 30, Philips, Eindhoven, Netherlands). A few milligrams of a powder were dispersed in 10 to 15 ml of isopropanol (>99.5 %, Fluka, Switzerland), and a few drops of the dispersion were applied on a copper grid coated with a carbon film (200 mesh, Plano GmbH, Wetzlar, Germany) and dried in a drying oven at 60 °C.

Refractive index (RI) of the powders was determined using the Becke Line Method [20]. Powder grains were embedded in immersion oils of known refractive index (Cargille Labs, USA). When focused in a light microscope a light seam at the edge of the grain can be observed and by defocusing the light seam moves either into or out of the grain. By increasing the distance between object and objective the seam moves to the material with higher refractive index and to the one having lower refractive index by reducing the distance. That way the refractive indices of immersion oil and powder can be matched iteratively until no movement of the light seam can be observed any more. Then the refractive index of the powder in question corresponds with the refractive index of the immersion oil. The accuracy of measurement is given by the step size and accuracy of immersion oils used and was 0.002 in this work.

8.4.3. Preparation of coatings

A commercially available two pack polyurethane system (Desmophen 800, Desmodur N3300, Bayer AG, Germany) was chosen as model coating system. The refractive index of the cured coating was determined by the Becke Line Method and shows a value of 1.512. A mixed oxide powder composition with 40 wt% alumina shows the same refractive index and was produced in bigger amounts. Coating formulations with 10 and 20 wt% of these RI matched nanoparticles were prepared and also ones with RI matched particles and dispersing additive (Disperbyk 161). For comparison coating formulations with a commercially available silica nanopowder (Aerosil OX50, Degussa, Germany) that has a refractive index of 1.46 and a difference to our coating system of 0.052 was prepared. Coatings were applied on object glasses using a 120 μ m doctor blade and cured in a heating oven for one hour at 80 °C before measuring transmittance.

8.4.4. Characterization of cured coatings

UV-vis spectra of cured coating films were recorded to determine the relative transmission. These spectra were recorded in the range between 300 and 800 nm using a UV-vis Spectrophotometer (Cary 50 Scan, Varian). An unfilled coating was measured to set the value for 100 % transmission.

Several coating samples were ultramicrotomed to determine the dispersion quality of nanoparticles in the coating layer. TEM images of these ultramicrotomed slices were recorded using a Philips CM 30 TEM.

Acknowledgements

Financial support by CTI (commission for technology and innovation) is kindly acknowledged (project KTI 7351.2). This work was also supported by the National Center of Competence in Nanoscale Science and the Swiss National Science Foundation. Very special thanks go to Ursula Sauder and Vesna Olivieri from the Microscopy Center at the University of Basel, Switzerland, for preparing innumerable samples for TEM investigation. Supporting Information is available online from Wiley InterScience or from the author.

References

- [1] S. C. Tjong, *Mat. Sci. Eng. R* **2006**, 53, 73.
- [2] L. Schadler, L. Brinson, W. Sawyer, *JOM* **2007**, 59, 53.
- [3] C. Chen, R. S. Justice, D. W. Schaefer, J. W. Baur, *Polymer* **2008**, 49, 3805.
- [4] B. Wetzler, F. Hauptert, M. Qiu Zhang, *Compos. Sci. Technol.* **2003**, 63, 2055.
- [5] C. Zilg, R. Müllhaupt, J. Finter, *Macromol. Chem. Physic.* **1999**, 200, 661.
- [6] H. Althues, J. Henle, S. Kaskel, *Chem. Soc. Rev.* **2007**, 36, 1454.
- [7] J. L. H. Chau, C.-C. Hsieh, Y.-M. Lin, A.-K. Li, *Prog. Org. Coat.* **2008**, 62, 436.
- [8] H. Schulz, L. Mädler, S. E. Pratsinis, P. Burtscher, N. Moszner, *Adv. Funct. Mater.* **2005**, 15, 830.
- [9] V. Khrenov, M. Klapper, M. Koch, K. Müllen, *Macromol. Chem. Physic.* **2005**, 206, 95.
- [10] B. Jauregui-Beloqui, J. C. Fernandez-Garcia, A. Cesar Orgiles-Barcelo, M. Mar Mahiques-Bujanda, J. M. Martin-Martinez, *Int. J. Adhes. Adhes.* **1999**, 19, 321.
- [11] M. A. Pérez-Limiñana, A. Torró-Palau, A. C. Orgilés-Barceló, J. M. Martín-Martínez, *Macromol. Symp.* **2003**, 194, 161.
- [12] C. Gerthsen, D. Meschede, in *Physik*, Springer, Berlin, **2005**.
- [13] H. Scholze, in *Glas*, Springer, Berlin, **1988**.
- [14] W. Stöber, A. Fink, *J. Colloid. Interf. Sci.* **1968**, 26, 62.
- [15] D. Bravo-Zhivotovskii, S. Melamed, Y. Apeloig, A. Schmidt, S. Melchior, G. E. Shter, G. S. Grader, *Chem. Mater.* **2001**, 13, 247.
- [16] A. Vital, A. Angermann, R. Dittmann, T. Graule, J. Topfer, *Acta Mater* **2007**, 55, 1955.
- [17] F. Bauer, H.-J. Glasel, U. Decker, H. Ernst, A. Freyer, E. Hartmann, V. Sauerland, R. Mehnert, *Prog. Org. Coat.* **2003**, 47, 147.
- [18] E. Barna, D. Rentsch, B. Bommer, A. Vital, O. von Trzebiatowski, T. Graule, *KGK-Kaut. Gummi Kunst.* **2007**, 60, 49.
- [19] M. Sabzi, S. M. Mirabedini, J. Zohuriaan-Mehr, M. Atai, *Prog. Org. Coat.* **2009**, 65, 222.
- [20] W. Kleber, in *Einführung in die Kristallographie*, (H.-J. Bautsch, J. Bohm), Verlag Technik, Berlin, **1998**.

9 Conclusion

The current work shows different synthesis routes to transparent nanocomposite films with improved scratch resistance. The aim was to identify the main parameters leading to improved scratch resistance without deterioration of optical properties.

The organosilanes surface modification of flame synthesised silica, alumina and titania nanoparticles was successful in the case of silica and alumina nanoparticles. It was shown that the different silanes were chemically bonded to the particle surface. For titania nanoparticles the silane molecules bound to the OH groups on the particle surface was poor in comparison with results obtained with silica and alumina nanoparticles.

These surface coated nanoparticles were incorporated in two polyurethane coating compositions and films made thereof. All nanoparticle filled samples showed improved scratch resistance compared to the unfilled references. Among silica particles best results were obtained with particles bearing a functional silane coating. TEM investigation showed a uniform dispersion, in particular for alumina nanoparticles. In the case of alumina also uncoated nanoparticles lead to surprisingly good scratch properties indicating a reaction of the isocyanate hardener with OH groups on the particle surface.

Commercial silica sols were also able to improve the scratch resistance of the coating systems but results were marginal in comparison with the reinforcement achieved by flame synthesized nanoparticles. However, good results were obtained with Nissan MIBK-ST particles and the synthesis of nanocomposites with organosols is fast and simple.

In a different approach tailor made mixed oxide nanoparticles with the same refractive index like the polymer matrix were successfully synthesised and incorporated in the polyurethane matrix. These nanocomposites showed improved film transparency.

Finally, we come to the conclusion that the main parameter influencing the scratch resistance of nanoparticle filled polymer coatings is the particle dispersion in the matrix. We also found that a good transparency of the resulting nanocomposite is an additional benefit of uniform particle dispersion. The scratch resistance can be further optimised by reactively linking the nanoparticles to the polymer matrix.

Curriculum Vitae

Elisabeth Barna

Dipl.-Ing.

* 07.04.1976 in Oberwart, Austria

Nationality: Austria

EDUCATION

01/2005 – 08/2010 PhD in Physical Chemistry, University of Basel, Switzerland

Supervisors: Prof. Dr. Wolfgang P. Meier, University of Basel, Switzerland
Prof. Dr. Andreas Taubert, University of Potsdam, Germany
Prof. Dr. Thomas Graule, EMPA, Switzerland

Topic: „Synthesis and characterisation of scratch resistant polyurethane clear coatings by incorporation of surface modified nanoparticles”

carried out in cooperation with EMPA – Federal Institute for Material Testing and Research, Dübendorf, Switzerland

10/1994 – 06/2003 Master of Science in Polymer Engineering and Science, University of Leoben, Austria

Supervisor: Prof. Dr. Klaus Lederer, University of Leoben, Austria

Topic: „Optimization of the compounding and mechanical properties of NBR nanocomposites based on surface modified layered silicates

WORK EXPERIENCE AND INTERNSHIPS

- since 01/2009 **Material Scientist**
HUBER+SUHNER AG, Pfäffikon ZH, Switzerland
- 03/2004 – 10/2008 **Research assistant and PhD Student**
EMPA - Federal Institute for Material Testing and Research,
Dübendorf, Switzerland
- Synthesis and characterization of nanocomposites based on polyurethane clear coating systems
 - Nanoparticle synthesis and silane surface modification
 - Mechanical characterisation and scratch testing, Transmission electron microscopy (TEM)
- 07/2001 - 12/2001 **Diploma student**
HUBER+SUHNER AG, Pfäffikon ZH, Switzerland
- Development of NBR nanocomposites based on layered silicates for roller application
 - Compounding and mechanical testing
- 07/2000 - 09/2000 **Internship**
HUBER+SUHNER AG, Pfäffikon ZH, Switzerland
- Development of polymer nanocomposites based on layered silicates for the application in cable insulation
 - Compounding and mechanical testing
- 07/1999 - 09/1999 **Internship**
07/1998 - 09/1998 **Ciba Specialty Chemicals AG, Basel, Switzerland**
- Electrical testing of resins
 - Development of a setup for low temperature $\tan\delta$ -measurements
- 08/1997 - 09/1997 **Internship, Plansee AG, Reutte, Austria**
- 07/1996 - 08/1996 **Internship, Dachstein - Kneissl GesmbH, Kufstein, Austria**
- 04/1996, 07/1995 and 04/1994 **Internship, Austrotherm GmbH, Pinkafeld, Austria**

POSTERS AND CONFERENCES

- 09/2005 NanoEurope, St. Gallen, Switzerland**
Poster: Surface modified nanoparticles for scratch resistant clear coatings
Elisabeth Barna, Bastian Bommer, Jürg Kürsteiner, Andri Vital, Oliver v. Trzebiatowski, Walter Koch, Bruno Schmid, Thomas Graule
- 10/2005 EMPA PhD Symposium, Dübendorf, Switzerland**
Poster: Surface modified nanoparticles for scratch resistant clear coatings
Elisabeth Barna, Bastian Bommer, Jürg Kürsteiner, Andri Vital, Oliver v. Trzebiatowski, Walter Koch, Bruno Schmid, Thomas Graule
- 05/2006 Nanotechnologie – Chance für den Korrosionsschutz, EMPA, Dübendorf, Switzerland**
Talk: Surface modified nanoparticles for scratch resistant lacquers
Elisabeth Barna, Bastian Bommer, Jürg Kürsteiner, Andri Vital, Oliver v. Trzebiatowski, Walter Koch, Bruno Schmid, Thomas Graule
- 06/2006 Funktionale Füllstoffe – Präparation und Verstärkungsmechanismen, DIK Hannover, Germany**
Talk: Surface modified nanoparticles for scratch resistant lacquers
Elisabeth Barna, Bastian Bommer, Jürg Kürsteiner, Andri Vital, Oliver v. Trzebiatowski, Walter Koch, Bruno Schmid, Thomas Graule
- 07/2007 International Conference on Composites and Nano Engineering, ICCE 15, Hainan Island, China**
Talk: Effect of Organosilane Grafted Nanoparticles on the Nano Scratch Resistance of Polyurethane Clear Coatings
Elisabeth Barna, Gregor Hünnebeck, Wolfgang Meier, Thomas Graule
- 08/2007 Eurofillers 2007 – Functional Fillers for Advanced Applications, Zalakaros, Hungary**
Talk: Impact of organosilane grafted nanoparticles on the scratch resistance of polyurethane clear coatings
Elisabeth Barna, Gregor Hünnebeck, Wolfgang Meier, Thomas Graule
- 07/2009 International Conference on Composites and Nano Engineering, ICCE 17, Honolulu, Hawaii, USA**
Talk: Synthesis and application of silica/alumina mixed oxide nanoparticles for transparent polyurethane nanocomposites
Elisabeth Barna, Andri Vital, Christian Weiher, Wolfgang P. Meier and Thomas J. Graule

SCIENTIFIC PUBLICATIONS

Surface Modification of Nanoparticles for Scratch Resistant Clear Coatings. KGK-Kaut. Gummi Kunst. 2007; 60 (1/2): 49. Barna E, Rentsch D, Bommer B, Vital A, von Trzebiatowski O, Graule T.

Synthesis of spherical, non-aggregated silica nanoparticles for nanocomposite coatings. KGK-Kaut. Gummi Kunst. 2005; 58 (5): 252-255. Graule TJ, Barna E, Bommer B, Kursteiner J, Vital A, von Trzebiatowski O, Schmid B, van Leeuwen J, Koch W.

Innovative, scratch proof nanocomposites for clear coatings. Compos. Part A-Appl. S. 2005; 36 (4): 473-480. Barna E, Bommer B, Kursteiner J, Vital A, Trzebiatowski O, Koch W, Schmid B, Graule T.

in progress

Scratch behaviour of polyurethane clear coatings reinforced with organosilane grafted nanoparticles
E. Barna, G. Hünnebeck, T. Graule, W. Meier

Efficiency of commercially available silica organosols in the scratch resistance improvement of transparent polyurethane clear coatings

E. Barna, A. Mielke, T. Graule, W. P. Meier

Refractive index matching of silica/alumina mixed oxide nanoparticles for scratch resistant clear coatings

E. Barna, A. Vital, C. Weiher, W. P. Meier, T. Graule

REFERENCES

Prof. Dr. Wolfgang P. Meier
University of Basel
Institute of Physical Chemistry
4056 Basel, Switzerland
Tel.: +41 (0)61 2673802
wolfgang.meier@unibas.ch

Prof. Dr. Thomas Graule
EMPA – Swiss Federal Institute for Materials Testing and Research
Laboratory for High Performance Ceramics
Ueberlandstrasse 129
8600 Dübendorf, Switzerland
Tel.: +41 (044) 832 4123
thomas.graule@empa.ch

Prof. Dr. mont. Clemens Holzer
Institut für Kunststoffverarbeitung
Montanuniversität Leoben
8700 Leoben, Austria
Tel.: +43 (0)3842 3501
Clemens.Holzer@unileoben.ac.at